THE EFFECT OF MICROSTRUCTURE ON THE FATIGUE CRACK PROPAGATION BEHAVIOR OF AN ALUMINUM-ZINC-MAGNESIUM-ZIRCONIUM ALLOY

A THESIS

Presented to

The Faculty of the Division of Graduate Studies

by

Edward James Coyne, Jr.

In Partial Fulfillment

of the Requirements for the Degree

Master of Science in Metallurgy

Georgia Institute of Technology

March, 1977

THE EFFECT OF MICROSTRUCTURE ON THE FATIGUE CRACK PROPAGATION BEHAVIOR OF AN ALUMINUM-ZINC-MAGNESIUM-ZIRCONIUM ALLOY

Approved:

Dr. Edgar A. Starke, Jr., Chairman

Dr. Saghana B. Chakrabortty

Dr. Miroslav Marek

Date approved by Chairman 3/3/77

TABLE OF CONTENTS

ACKNOWLEDGEMENTS

The author would like to express his sincere appreciation to his thesis advisor, Dr. E.A. Starke, Jr. whose invaluable guidance made this work possible. He also wishes to thank Dr. S.B. Chakrabortty and Dr. M. Marek for their helpful suggestions in reviews of this work

The helpful advice and assistance of Dr. S. Spooner during the computer analysis is deeply appreciated. Mr. Charles Blackwood of the Chemical Engineering and Metallurgy Machine Shop deserves much credit for the preparation of samples. The assistance of Danny Averette in the machine shop is appreciated.

The author would like to thank his wife, Darlene, for her support, assistance, faith and typing during this project. He would also like to thank his parents for their interest and support during this work.

The author would also like to thank his colleagues for their assistance and support throughout this project.

The author would like to thank the Alcoa Technical Center for preparing the alloys used in this investigation. The financial support of the Alcoa Foundation and St. Joe is appreciated.

LIST OF ILLUSTRATIONS

Figure Page

Figure Page

LIST OF TABLES

SUMMARY

The effect of microstructure on the fatigue crack growth behavior of an Al-Zn-Mg-Zr alloy was investigated. The fatigue crack behavior was compared to the previously obtained low cycle fatigue behavior of the same alloy. The major effect of the microstructure on the fatigue crack propagation rates was found at the low stress intensity ranges. At these stress intensity levels the overaged condition was found to have lower crack growth rates. This improved fatigue resistance was attributed to the increased homogeneity of deformation resulting from the occurrence of dislocation looping as the primary deformation mode. At the intermediate stress intensity levels tested, there was little, if any, effect of microstructure.

A correlation was attempted between the observed data and the crack growth rates predicted by some proposed fatigue crack growth laws. The proposed laws that contain a variable power dependence for the stress intensity factor predicted the crack growth rate with extreme accuracy. Laws which had a fixed power dependence for the stress intensity factor did not accurately predict the observed crack growth rate.

Values of the parameters in the fatigue crack propagation equations were found to correlate with the cyclic low cycle fatigue parameters. No correlation was found between monotonic tensile parameters and the fatigue crack law parameters.

CHAPTER I

INTRODUCTION

The fatigue process may be described as the progressive development of a crack from the submicroscopic phases of cyclic slip and crack initiation, through the macroscopic crack propagation period to the final fracture[1]. The high strength aluminum alloys have been found to possess very poor fatigue properties[2]. Improvements in the fatigue resistance of these alloys lie in the ability to produce metallurgical structures which resist the formation of microstructural instabilities which can lead to fatigue crack initiation and which are also resistant to subsequent fatigue crack growth[3].

In high purity Al-Zn-Mg alloys fatigue cracks have been observed to travel in an intergranular fashion in moist test environments. However, the introduction of Cr, Zr, Ti, etc. as grain refiners results in either smaller grain sizes and a less uniform grain surface or unrecrystallized or partially recrystallized structures. This is expected to make grain boundary fatigue crack propagation (FCP) more difficult[4]. However any major alloying change to improve the fatigue crack growth resistance must not be done at the expense of other properties, such as stress corrosion cracking resistance or resistance to fatigue crack initiation[3].

Microstructural changes, as a result of aging, have been

shown to affect the low cycle fatigue (LCF) properties in Al-Zn-Mg (-Zr) alloys[5,6] and fatigue crack growth rates in 2xxx and 7xxx alloys[2,3]. The purpose of this study was to investigate the effects of variations in the aging times (and thus the strengthening agent type and size) on the fatigue crack propagation rates in an Al-Zn-Mg-Zr alloy, and to determine if a correlation can be made between the FCP data and previously obtained LCF data[6].

CHAPTER II

REVIEW OF THE LITERATURE

Factors Governing Fatigue Crack Growth

Numerous factors affecting crack propagation rates have been studied[1,3,7-25]. Forman[7] suggests a large number of variables which must be considered during numerical analysis of crack growth data. Some of these factors will be discussed while others will only be listed.

Stress intensity seems to be the major factor affecting crack growth rates. The growth rate increases as the stress intensity increases, but the relationship between them is uncertain. The effect of all other factors, e.g. environment, is usually presented for a given stress intensity range. Environmental factors play a decisive role in FCP. Moisture[1,3,8-12] and temperature[1,9] can alter the crack growth rate by a factor of ten[9]. Hahn and Simon[8] found that crack growth differences can generally be traced to the moisture content in the air or the corrosive effect of the water vapor. Wei[9] and Broom and Nicholson[11] correlate this effect with diffusion, ionic formation, and diffusion and recombination of ions at the crack tip. Hartman[10] found this effect to be more pronounced at low ΔK ranges. Wei[9] and Walton and Ellision[1] have found that temperature also affects the crack growth rate. They observed that an increase in temperature will produce an increase

in crack growth rate at the same ΔK range and Wei has developed a crack growth law which includes this parameter[9].

Some material parameters are important factors affecting crack growth rate. Forman[7] used the critical stress intensity factor for fracture, K_c, in his crack growth equation. Young's modulus, E, has been suggested as the dominate material parameter affecting propagation rates[13]. Several investigators[13-16] have included this parameter in their crack growth laws. Hickerson and Hertzberg[17] state that while the factors controlling the material constants in the Paris equation (see Equations and Laws section) are not well known, the existing data indicates that changes in E inversely affect the growth rate at equivalent ΔK values. Other material parameters which have been found important are the yield strength[15,18], the yield strain[18] and the ultimate tensile strength[14].

Certain test variables affect the crack growth rates. Forman[7] first proposed that the load ratio, R, (minimum load/maximum load) needed to be considered in FCP testing. Hudson and Scardina[19] found that the rate of fatigue crack growth, at a given ΔK value, varied directly with the load ratio and that spreads in the growth rates at different R values became larger at larger ΔK values. They also found that the pre-exponential constant in the Paris equation depended on R. The other major experimental variable which has been found to affect crack propagation rates is the frequency at which the test is conducted. Hahn and Simon[8] found that crack growth differences can generally be attributed to the frequency dependence

of the corrosion which occurs in moist environments. A recent study at Alcoa[3] showed more scatter in the results in moist environments than in dry air when tests were conducted at different frequencies. However, the results did not consistently show whether crack rates increased or decreased as test frequency increased. Frost et al[20] state that the available evidence suggests that frequency has very little effect on growth rates characteristics over the range of 0.25-100 Hz and that the growth rate is likely to be slightly faster at lower frequencies. According to Forman[7] another testing variable that needs to be considered is the manner in which the specimen is loaded, that is, whether the load spectrum is triangular or sinusoidal. At present no investigation has been conducted in this area.

Crack behavior during a test affects propagation data, as does material response. Crack tunnelling, i.e. the crack being longer at the midsection of the sample than at the surface, has been observed[21]. This has been partially explained as cleavage fractures of brittle particles causing a difference in crack length at the surface from that in the interior[15]. The plane-strain to plane-stress transition occurs as the plastic zone size increases with increasing ΔK and crack growth rate[13]. This transition occurs as the plastic zone approaches the thickness of the specimen[13] and produces a sigmoidal shape in the da/dN va. ΔK plots[12]. This sigmoidal shape is also dependent on the purity of the alloy and on the corrosive nature of the test environment[12].

A significant amount of strain cycling occurs at the crack

tip during a FCP test[19]. The effect of strain cycling in the reversed plastic zone at the crack tip is to alter the mechanical properties e.g. the strain at the 0.2% offset yield and cyclic strain hardening. The material in the reversed plastic zone is best described by mechanical properties present following cyclic stabilization in strain cycling tests[17]. The rate of fatigue crack growth is basically dependent upon the cyclic stress-strain characteristics of the material since these characteristics control the size of the deformation zone ahead of the crack[22]. The effects of the crack surface, the crack growing out of the plane perpendicular to the loading direction, creep and relaxation, and fatigue crack initiation are factors which need to be investigated more fully.

The method of data processing, e.g. graphical, polynominal, or secant method[21], raw data (a versus N results) affects the scatter in results and calculated crack growth rates. The graphical method is very subjective and hence shows the most scatter. The secant method shows more variance than the polynominal method. The amount of variability increases when the raw data does not represent a smooth curve. Clark and Hudak[21] have done an extensive review of this variable and further discussion will not be presented here.

Effect of Microstructure on Fatigue Crack Propagation

The effect of composition and structure on crack growth rates is a major source of debate. Inclusions have been found to both enhance[23] and impede[24] crack growth. Forsyth[23] maintains that inclusions form small cracks in the plastic zone ahead of the

crack tip and that these small cracks ultimately link up with the main crack thereby accelerating the fatigue crack growth. McEvily[24], on the other hand, states that inclusions act as crack inhibitors by reducing the crack tip sharpness and leading to crack branching. Kershaw[25] states that the effect of these particles depends on the stress intensity range and that the effect changes as the ΔK range is increased. Researchers at Alcoa[3] have found that inclusions and constituent particles have no large effect on the crack growth rate and that the particles offer only local resistance to the advancing crack front at intermediate ΔK values. Coarse particles do not appear to be a factor in fatigue crack growth[26]. At low ΔK ranges the crack growth rate for alloys homogenized at high temperatures is slightly lower than for those homogenized at low temperatures[26]. The intermediate precipitate size is larger in the alloys homogenized at high temperatures and the precipitate spacing is larger. Consequently, at low ΔK vlaues, either the particle size or the interparticle spacing becomes important.

Grain size and grain boundary effects offer another area of contention. The intermediate precipitates have their strongest effect on the crack growth rate by the control of grain size, with a low density of large precipitates being preferable to a high density of small precipitates[26]. A recent study[26] shows that fatigue crack growth rate is linearly proportional to the grain diameter. Hahn and Simon[8] also found that grain boundaries represent larger obstacles to cyclic growth than grain interiors and that a sufficient number of grain boundaries in the path of the crack will reduce the

growth rate. Nageswararao et al[4] found crack growth to be a discontinuous process at grain boundaries in high purity aluminum. Alcoa researchers[3] report that grain size, and therefore the number of grain boundaries, have no effect on the crack growth rate.

Equations and Laws of Fatigue Crack Propagation

Many fatigue crack propagation (FCP) laws and equations have been derived theoretically and experimentally. Recent reviews of FCP equations[2,27] have described these various theories; only a few, demonstrating the different approaches taken to FCP, will be discussed.

The majority of investigators have found that the Irwin stress intensity factor, K, is a valuable parameter when trying to correlate crack growth data[17]. The K values can be obtained using the equation[28]:

$$K_I = Y.\frac{P\sqrt{a}}{BW} \qquad (1)$$

with, for specimens with a H/W ratio of 0.6,

$$Y = 29.60-185.5(\frac{a}{W})+655.7(\frac{a}{W})^2-1017(\frac{a}{W})^3+638.9(\frac{a}{W})^4$$

for $\frac{a}{W}$ = 0.3 to 0.7 and

$$Y = 23.12-67.67(\frac{a}{W})+97.31(\frac{a}{W})^2$$

for a/W = 0.4 to 0.6 where a is the crack length, W is the specimen width, K_I is the stress intensity for mode I loading, Y is the K calibration for compact tension specimens, B is the specimen breadth and P is the applied load. Paris[29] first expressed the dependence of crack growth on K as:

$$\frac{da}{dN} = C(\Delta K)^m \tag{2}$$

where ΔK equals the difference between the maximum and the minimum values of K and C and m are not parameters. Paris found that m = 4 for plates of infinite width loaded in uniaxial tension, mode I.

Forman et al[7] modified Paris' equation to take into account the load ratio, R, (minimum stress/maximum stress). Forman expressed this dependence as:

$$\frac{da}{dN} = \frac{C(\Delta K)^m}{(1-R)K_c - \Delta K} \tag{3}$$

where K_c is the critical stress intensity factor for fracture. Others[18,19,30] have correlated the effect of the mean cyclic stress and R on da/dN and tend to agree with Forman's contention that R is an important variable in determining crack growth rates.

Schwalbe[27] pointed out that existing FCP equations are based on two different assumptions. One assumption is that crack

propagation is directly related to plastic deformation at the crack tip. Advocates of this approach[14,20,22] base their crack growth equations on the value of the cyclic stress. For example, Lardner[14] states the crack rate as:

$$\frac{da}{dN} = \frac{\pi \cdot (1-\upsilon)}{4 \cdot G \cdot \sigma_1} \cdot \Delta\sigma^2 \tag{4}$$

where υ is Poissons ratio, G is the shear modulus and σ_1 is the resistance against plastic deformation. Using the relation $K = \Delta\sigma\sqrt{\pi a}$, equation 4 can be rewritten as:

$$\frac{da}{dN} = \frac{(1-\upsilon^2)}{2E \cdot \sigma} \cdot \Delta K^2 \tag{5}$$

using the ultimate tensile strength σ for σ_1. Lardner made this substitution since cyclic plastic deformation causes strain hardening in the material of the plastic zone.

A strain hardening model was originally hypothesized by Head[31]. The equation is expressed as follows:

$$\frac{da}{dN} = \frac{\beta}{12E} \frac{\sigma^2 a}{(\sigma_u - \sigma_{ys})\sigma_{ys}} \tag{6}$$

where β is the work hardening coefficient, a is the crack length, σ is the applied stress and σ_{ys} and σ_u are the yield and ultimate stress, respectively.

McClintock[32] used a Coffin-Manson type low-cycle fatigue damage law and developed a more detailed work hardening model. This model is expressed as follows:

$$\frac{da}{dN} = \frac{7.5}{\rho} \left(\frac{\varepsilon_y}{\varepsilon_f}\right)^2 R_p^2 \tag{7}$$

where $R_p = \frac{\pi}{8} \left(\frac{Kmax}{\sigma_{ys}}\right)^2$

with R_p and ρ being the plastic and process zone sizes respectively and ε_y and ε_f are the yield and fracture strains, respectively. The equation for R_p is similar to many proposed, but is the one due to Dugdale[33].

The second assumption on which crack propagation laws are founded is that crack propagation is the consequence of damage in the plastic zone caused by the cyclic plastic deformation. Weertman[15] and others[32,34] base their crack propagation laws on this assumption. Weertman found that a crack propagates when the sum of the cyclic plastic deformation at the crack tip reaches u*, the critical value of displacement for crack propagation. Weertman expresses the crack growth rate as:

$$\frac{da}{dN} = \frac{\pi \cdot (1+\upsilon)}{24 \cdot u^* \cdot \sigma_B} 3 \cdot E \cdot \Delta K^4 \tag{8}$$

Derivations of the fatigue crack growth rate from the first assumption yield a second power dependence on K, whereas those based on the second assumption concerning the damage criterion yield a fourth power dependence[27].

Crack growth rate equations combining microscopic factors with macroscopic factors have been proposed[35]. The plastic zone size at the crack tip at the maximum applied stress and the cyclic plastic zone size were related to crack growth rate by Erdogan[35] by:

$$\frac{da}{dN} = A\rho_{max}^{\alpha} \rho_{r}^{\beta} \tag{9}$$

where A, α and $\beta$are material constants, ρ_{max} is the plastic zone size at the crack tip corresponding to the maximum applied stress and ρ_r is the cyclic plastic zone size. Using local conditions around the crack tip Erdogan calculated the plastic zone sizes and obtained:

$$\frac{da}{dN} = B\left(\frac{1}{1-R}\right)^{2\alpha}(\Delta K)^{2(\alpha+\beta)} \tag{10}$$

where B is a material constant.

Kanazawa et al[18] deduced a FCP law from consideration of events occuring at the fatigue crack tip. The law is based on the absorbed hysteresis energy per stress cycle, I, at the crack tip. The main feature of this law is that the crack propagation rate is dependent only on the absorbed hysteresis energy, which includes

the effect of the stress ratio. The absorbed energy, I, can be expressed as:

$$I = 4\sigma_y \varepsilon_y \sqrt{\rho}_{max} \sqrt{\rho}_r \tag{11}$$

where σ_y and ε_y are the yield stress and strain, respectively. Crack growth rate dependence on I has been shown to be[15]:

$$\frac{da}{dN} = C(I)^m \tag{12}$$

where C involved an R dependence term:

$$C = f\left(\frac{1}{1-R}\right)^m \tag{13}$$

Ikeda et al[36] developed a theory along the same general lines.

Antolovich[37] proposed an equation relating low cycle fatigue results and fatigue crack growth rates. This equation is:

$$\frac{da}{dN} = 4\left(\frac{0.7\alpha}{E\sigma_{ys}(1-S)\varepsilon_f}\right)^{1/\beta}\left(\frac{1}{\ell^{1/\beta-1}}\right)(\Delta K)^{(2+S)/\beta} \tag{14}$$

with $\ell = \alpha(\Delta K/\sigma_{ys})^{(2+S)}\sigma_{ys}/E\varepsilon_f$

where ℓ is the process zone size, α is the numerical constant, S is a

small number (according to Antolovich), β is the Coffin-Manson exponent, ε_f is the monotonic fracture strain, and σ_{ys} is the monotonic yield strength. The numerical constant, α, has the units of length$^{-S/2}$ in order to make the units of the equation predict crack growth in length.

Theories based on the crack tip opening displacement (CTOD) consider crack growth to be a geometric result of the crack tip deformation. These theories are largely insensitive to the structure of the material and are based mainly on stress and strain distributions. Pelloux[16] considered his material to be an ideally rigid-plastic material and assumed that the crack tip maintained a 90^o angle to the tensile direction while opening in an alternating shear mechanism. This theory leads to a crack growth rate of:

$$\frac{da}{dN} = C(CTOD) = C\left(\frac{.25\Delta K}{\sigma_y E}\right)^2 \qquad (15)$$

which gives an upper limit for crack growth per cycle. Other equations using CTOD models have been proposed. Ikeda et al[36] proposed that all the plastic deformation contributing to crack growth occurs in a small area bounded by two lines making a sharp angle with the crack plane. Pook and Frost[37] postulated that the crack tip assumes an elliptical profile under stress. Threshold values for ΔK have also been proposed for CTOD-type equations[13].

The crack growth equations derived from different models, such as those based on plastic deformation in elastic materials, those

taking into account individual work hardening, and those based on using a strain distribution for purely elastic deformation all tend to agree with the experimental results with the same degree of accuracy[27].

The derivation of fatigue crack growth laws can not be exact since the crack tip behavior is not fully known. Also factors governing the growth rate, such as environment and temperature, make the derivation of exact laws difficult[27].

Fatigue Crack Behavior

Fatigue crack growth in aluminum alloys is found to generally occur in two stages, designated as Stage I and Stage II[39]. Stage I crack growth is initially along the crystallographic plane of maximum shear stress. Slip band extrusion is reportedly absent under conditions of repeated tension stress[40] but the crack still originates in slip bands[41]. Stage I fatigue cracks continue to grow along slip planes in the absence of sufficiently large tensile stress components. Stage I crack growth can be considered an extension of crack initiation and occupies a large portion of the life at low stresses[39]. As the crack lengthens the peak stress rises until microscopic deformation occurs at the fatigue crack tip causing fatigue striations to become resolvable on the fracture surface. When this occurs the crack ceases growing along the direction of maximum shear and begins travelling along a direction perpendicular to the direction of the applied stress[41]. This type of crack growth is designated as Stage II growth and accounts for most of the life at high stress amplitudes[36].

Fatigue crack propagation is, in part, a result of repeated cyclic extension by alternating shear[22], a mechanism of rupture playing an important role in fracture. This mechanism is limited due to subsequent blunting at the tip of the crack. This phenomenon is characterized by many slip markings parallel to the propagating crack front.

In a moist environment fatigue crack growth rates are accelerated[1,3,8-11]. This acceleration has been proposed[3] as due to an increase in the stress intensity factor at the crack tip. Broom and Nicholson[11] proposed that this increase in K is produced by a build up of hydrogen pressure in the internal 'voids' ahead of the existing crack front. The hydrogen pressure build up results from the formation of hydrogen ions by the reaction of water with the freshly created crack surfaces. The ions then diffuse to an internal surface and recombine, causing an increase in pressure and hence in stress.

The crack path depends on the purity of the alloy, the environment, and the aging condition in Al-Zn-Mg alloys[4]. In high purity samples aged to maximum hardness and tested in a moist environment, the crack was found to propagate along grain boundaries. The grain boundaries were so weak that the crack was sometimes observed to propagate transgranularly for a short distance and then suddenly bypass the grain interior and travel along the nearest grain boundary. In overaged, high-purity samples the crack usually propagated transgranularly in either a moist or dry environment. Crack propagation was found

to be a discontinuous process in the high purity samples. Commercial purity alloys were found to fail transgranularly in either a dry or moist environment. The presence of Cr, Zr, Ti, etc. as grain refiners caused transgranular fracture in the high purity alloys[4], however constituent particles have no effect on the crack path of aluminum alloys[3] and offer only local resistance to the advancing crack.

The contribution of the inclusions to the crack growth rates should best be assessed by measuring the fraction of the fracture surface caused by local voids or ductile tearing around inclusions rather than by comparing the fatigue striation spacings to the macroscopic growth rates[12]. Fracture surfaces found at low ΔK testing of aluminum using scanning electron microscopy, appear much flatter than those obtained at higher ΔK vlaues. No evidence of fatigue striations is evident for the low ΔK tests[3]. The Stage II crack growth[39] gives the fatigue striations often characteristic of FCP tests. Differences in the fatigue striations and the macroscopic crack rates have been observed in aluminum alloys[8]. Cleavage fracture of brittle particles has been offered as a partial explanation of this discrepancy[25] but the origin of the discrepancy or the purity levels necessary to bring the macroscopic growth rate and the striation spacings into line are yet to be established for aluminum alloys[8]. As the ΔK range increases, the agreement between the surface cracks and the striation spacings becomes less[25].

In many cases this inherent scatter in crack growth data is enough to prevent the ranking of fatigue crack growth rates of different alloys and heat treatments. However for this study heat treatments

have been selected to enable a study of the alloy in the three most differing conditions, i.e. very underaged, aged to maximum strength and grossly overaged. This should enable a study of several effects, e.g. yield strength, particle size, and low cycle fatigue properties, on the fatigue crack propagation rates.

CHAPTER III

EXPERIMENTAL PROCEDURES

Following a recent investigation of the low cycle fatigue properties of Al-Zn-Mg alloys[5] a study[6] was made to determine the effect of adding a grain refiner, Zr, to the ternary alloy on these properties. It was determined that the small grained Al-Zn-Mg-Zr alloys performed better in low cycle fatigue than did the large grained ternary[6]. In view of this fact the Al-Zn-Mg-Zr alloy was chosen for this fatigue crack propagation study in order to determine if there is a relationship between the condition best suited for low cycle fatigue (LCF) and for fatigue crack propagation (FCP).

The alloy studied in this research was prepared at the Alcoa Technical Center, Alcoa Center, Pennsylvania. The mechanical and thermal treatments used in producing the alloy are considered proprietary by Alcoa and as such can not be detailed here. The alloy was received in plate form. The composition (in weight percent) of the Al-Zn-Mg-Zr alloy is presented in Table I, along with that of the ternary alloy used in the previous study.

The plate was cut into sections 4.57 cm. by 4.70 cm., with the rolling direction parallel to the 4.70 cm. side. The sections of plate were solutionized for 1 1/2 hours at 480^{o}C and quenched in ice brine. Following solutionization the samples were directly

Table 1. Composition of the Aluminum Alloys

	Si	Fe	Cu	Mn	Mg	Cr	Zn	Ti	Be	Zr
Al-Zn-Mg	0.00	0.00	0.00	0.00	2.20	0.00	6.17	0.00	0.00	0.00
Al-Zn-Mg-Zr	0.05	0.04	0.01	0.00	2.08	0.00	6.45	0.02	0.00	0.11

transferred to a constant temperature oil bath for aging. The different aging treatments are presented in Table II. Samples of each aging treatment, the as-received and the solutionized condition were polished for metallographic examination of the three principle sections of the plate.

Fatigue crack propagation samples, compact tension type, were cut from the heat treated sections, with the starter notch cut perpendicular to the rolling direction and a crack plane orientation L-T, Figure 1. The specimens were kept refrigerated between heat treating and machining and testing to prevent further natural aging from occurring. Before testing one side of each sample was ground and polished to a .3μ finish to facilitate observation of the crack during testing. The crack propagation tests were performed on a closed loop servohydraulic Materials Testing System (MTS) using a tension-tension loading with a minimum-maximum load ratio of 0.1, at a frequency of 5Hz. The tests were carried out in laboratory air with a relative humidity of 27-30% and a temperature of 23-25^{o}C. The crack length was measured using a Gaertner travelling microscope to within ±0.01 mm. A minimum of four samples from each aging condition were tested.

Scanning electron microscopy samples were prepared from the fatigue propagation samples after failure. The FCP specimens were sectioned 4-6 mm. below the fracture surface and the starter notch section removed. The scanning electron microscopy was done on a CWIKSCAN/100 Field Emission Scanning Microscope at 16.5KV.

A computer analysis was conducted on the crack growth data.

Table 2. Effect of Aging Treatment on Precipitate Size in Al-Zn-Mg-Zr and Al-Zn-Mg Alloys

Aging Treatment Designation	Aging Time (hrs) 120°C	Aging Time (hrs) 150°C	Guinier Radius (Å) Al-Zn-Mg-Zr	Guinier Radius (Å) Al-Zn-Mg*
Underaged	4	-	-	25
Double Aged	2	12	29	-
Overaged	-	24	-	71

* From work of Sanders[5] on Al-Zn-Mg.

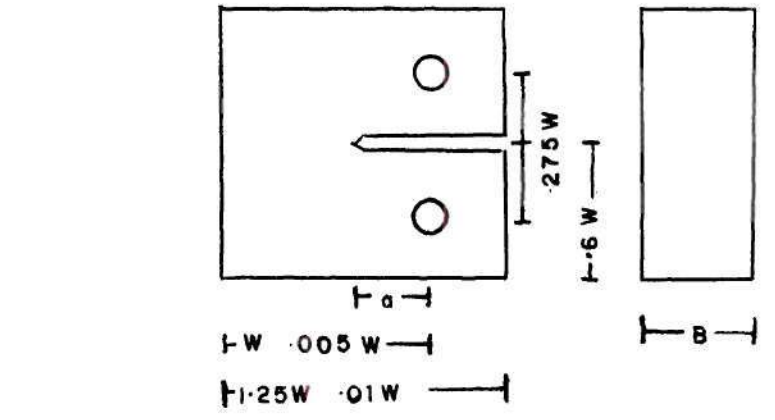

W = 38.1 mm.

B = 6 mm.

Hole diameter = W/4

H/W = .6

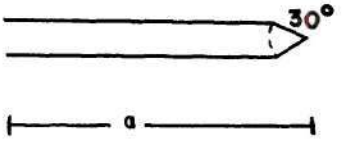

Width of crack starter notch
must not be greater than W/10

Figure 1. Compact Tension Specimen Used for Fatigue Crack Propagation Tests.

A linear regression least squares fit was performed on the raw da/dN vs. ΔK data. The smooth line data was used to test previously proposed equations for predicting crack growth, especially those using low cycle fatigue parameters. The unknown parameters in the growth rate prediction formulas were found using a Chi-squared technique.

CHAPTER IV

EXPERIMENTAL RESULTS

The solution treatment, i.e. 1 1/2 hours at 480°C, of the as-received Al-Zn-Mg-Zr alloy produced a partially recrystallized microstructure. The large variation of grain size and grain shape made exact determinations of the grain dimensions impossible, but approximate mean grain dimensions were 0.03mm X 0.05mm X 0.10mm[6]. The as-received, solutionized and maximum strength microstructures are shown in Figures 2 to 4. Small intermetallic paricles were found running in the rolling direction of the plate. These particles were probably Al-Fe-Si[26], formed as the result of the presence of 0.05% Si and 0.04% Fe in the alloy.

The effect of altering the aging times and temperatures on the precipitate size and type has been previously determined using x-ray small angle scattering (XSAS) for the Al-Zn-Mg[5] and Al-Zn-Mg-Zr[6] alloys. It was found that the 0.1 percent zirconium did not alter the precipitation sequence or aging kinetics. The zirconium is precipitated as stable Al_3Zr particles which are 0.1μ in diameter[26] after solutionization and should not be altered during aging. The double aging treatment of 2 hours at 120°C and 12 hours at 150°C procuced a microstructure of mostly η'[42] and probably some η($MgZn_2$), having a R_G = 30Å. Aging for 4 hours at 120°C produced coherent Guinier-Preston zones having a R_G = 25Å[43]. Larger, partially coherent η' and incoherent η particles with a R_G = 71Å[43]

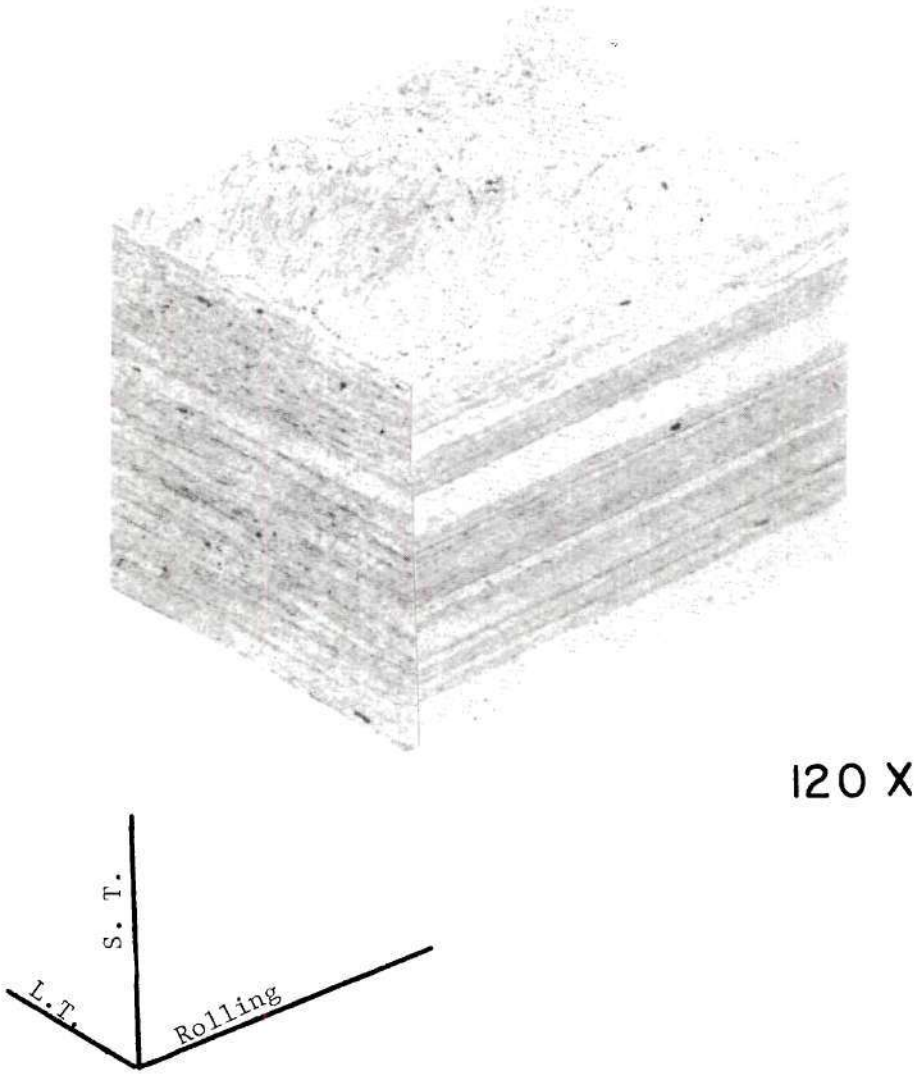

Figure 2. Microstructure of Al-Zn-Mg-Zr Plate in the As-received Condition. Keller's Etch.

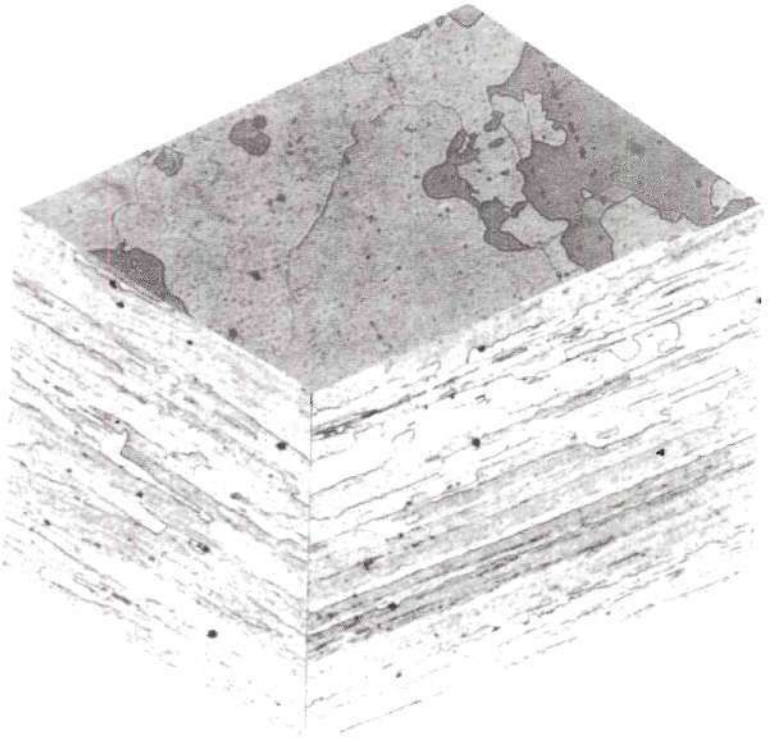

120X

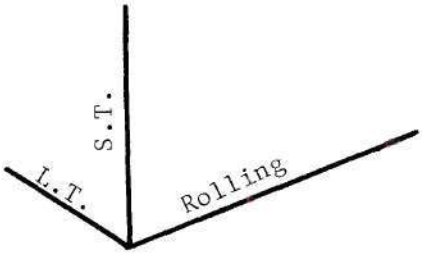

Figure 3. Microstructure of Al-Zn-Mg-Zr Plate After Solutionizing at 480°C for 1 1/2 hours. Keller's Etch.

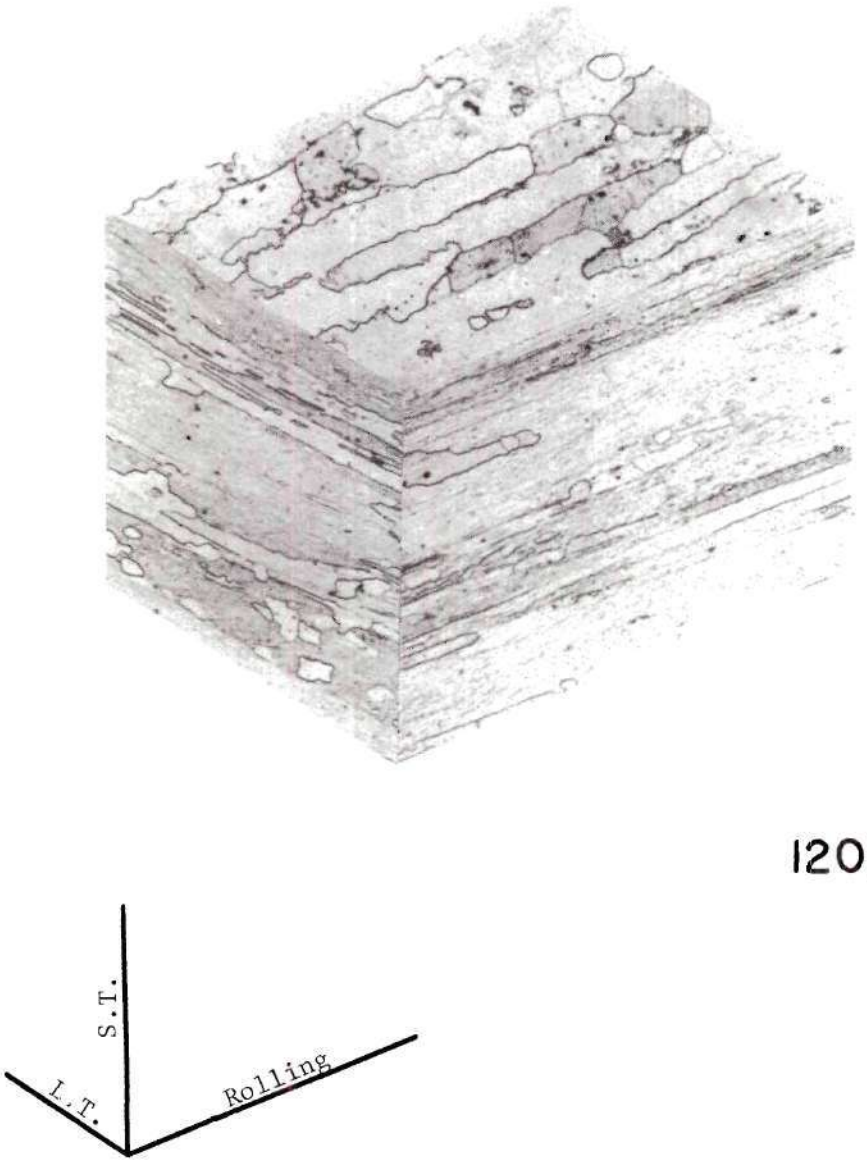

Figure 4. Microstructure of Al-Zn-Mg-Zr Plate After Aging for 2 hours at 120°C and 12 hours at 150°C. Keller's Etch.

were produced by the 24 hours at 150°C aging treatment. Table 2 shows the radii of gyration (R_G), calculated from the Guinier approximation, for the Al-Zn-Mg-Zr alloy[44] as well as the data for an Al-Zn-Mg alloy[43].

The monotonic and low cycle fatigue properties of the Al-Zn-Mg-Zr alloy are presented in Table 3[6]. The yield strengths of the underaged and overaged conditions are similar, 368 and 378 MNm^{-2} respectively, and the yield strength of the double aged condition is 445 MNm^{-2}. The ultimate strength was the lowest for the overaged condition and highest for the double aged condition. The work hardening exponents, n, increase with the yield strength and the true strains fracture, ε_f, decrease with the yield strengths. The cyclic work hardening exponent, n', increases as the aging proceeds from an underaged condition to a double aged and then overaged condition. In the high strain region the Coffin-Manson exponents, -C, increase with ultimate strengths and the low cycle fatigue ductility coefficients, ε_f', increase with yield strengths. In the low strain region -C and ε_f' increase as the cyclic work hardening exponent.

The path by which the crack propagated, with respect to the grain structure, is shown in Figure 5. The crack appears to follow an intergranular path when grain boundaries are readily available. However, when grain boundaries are absent in the close proximity of the crack tip the crack will travel transgranularly. When the crack travels transgranularly it does so in a straight line, but this straight line may change directions at grain boundaries.

Considerable branching occurred in the fatigue cracks grown

Table 3. Tensile and Cyclic Properties of Al-Zn-Mg-Zr

Sample	Tensile				Cyclic		
	Yield MN/m^2	UTS MN/m^2	n	ε_f(%)	-C	n'	ε_f'(%)
Underaged	368	441	.050	17.2	.62	.086	43
Double Aged	445	469	.013	12.9	.71	.092	98
Overaged	378	412	.030	14.3	.48 .92	.102	48 632

Crack direction

(a)

330X

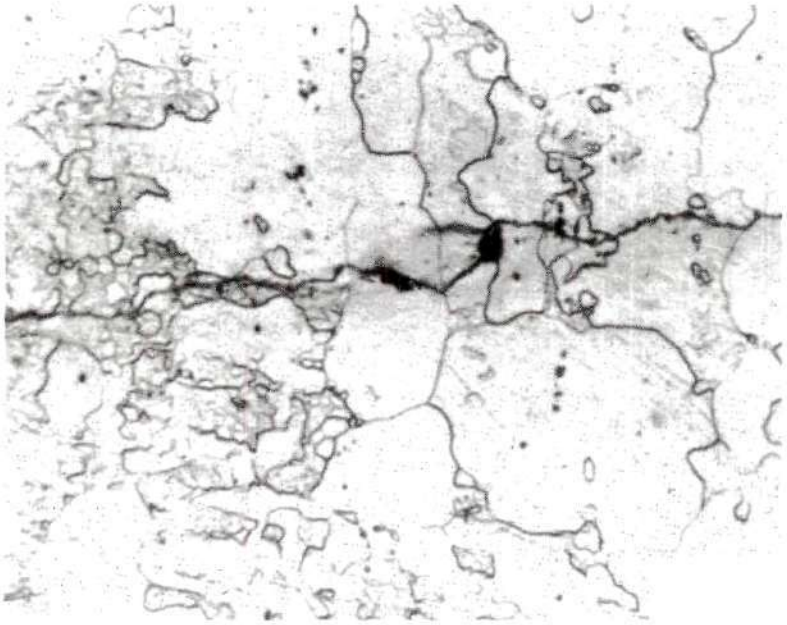

200X

(b)

Crack direction

Figure 5. The Path of Crack Propagation with Respect to the Grain Structure: (a) underaged, and (b) double aged.

in the samples double aged 2 hours at 120°C and 12 hours at 150°C, Figure 6. Although crack branching is a good means of crack retardation, in cases where the branching caused a noticeable degree of retardation the results of the crack growth test, following the branching, were ignored since the effective ΔK level for the test was no longer the calculated value. The applied stress was then being distributed over multiple crack fronts, rather than one, and hence the propagation energy was being spread over multiple crack tips.

The fatigue crack growth rate data are shown in Figures 7 through 10 in the conventional da/dN vs. ΔK plots. Part (a) the low ΔK straight line portion of the da/dN vs. ΔK plots, part (b) the intermediate ΔK portion of the plot and part (c) of each figure shows the entire experimental plot. The ΔK values were obtained from the difference of the calculated K_{Imax} and K_{Imin}. For the straight line portion of each plot at low ΔKs a straight line was placed through the data using a least squares fit. The intermediate ΔK section of plots was assumed to be a straight line for data correlations. Although this assumption is not completely valid, the line obtained closely approximates the data. The intermediate ΔK region line was also obtained using a least squares fit. The upper ΔK section line was drawn through the data by examination. This section of the data had few data points since the crack growth was rapid and because this portion of the curve was not of primary concern in this work. Table 4 shows a comparison of crack growth rates for given values of ΔK for the three heat treatments.

A correlation between the observed crack growth rates and those

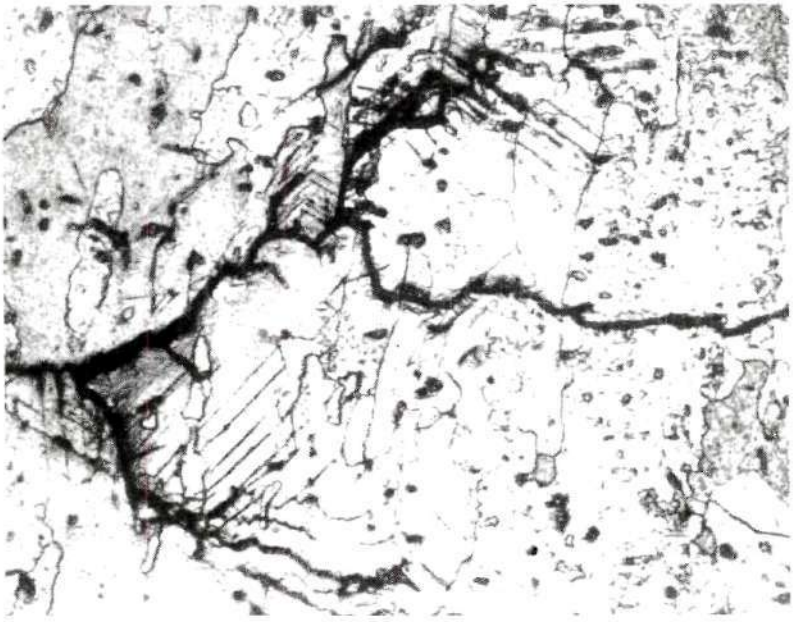

Crack direction

220X

Figure 6. Crack Branching in the Underaged Condition.

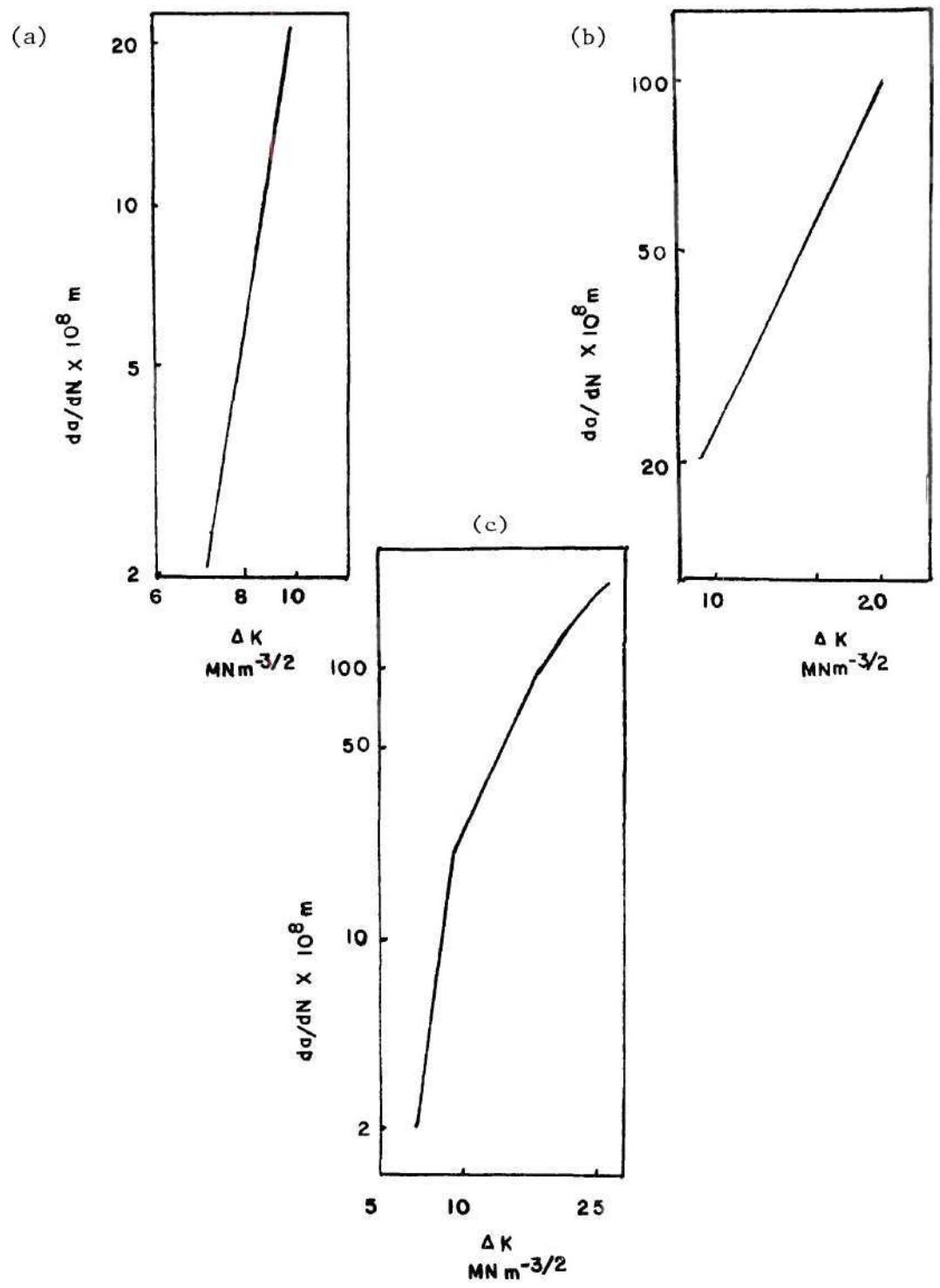

Figure 7. Fatigue Crack Growth Plots, da/dN vs. ΔK, for the Overaged Condition: (a) low ΔK range, (b) intermediate ΔK range, and (c) entire crack growth plot.

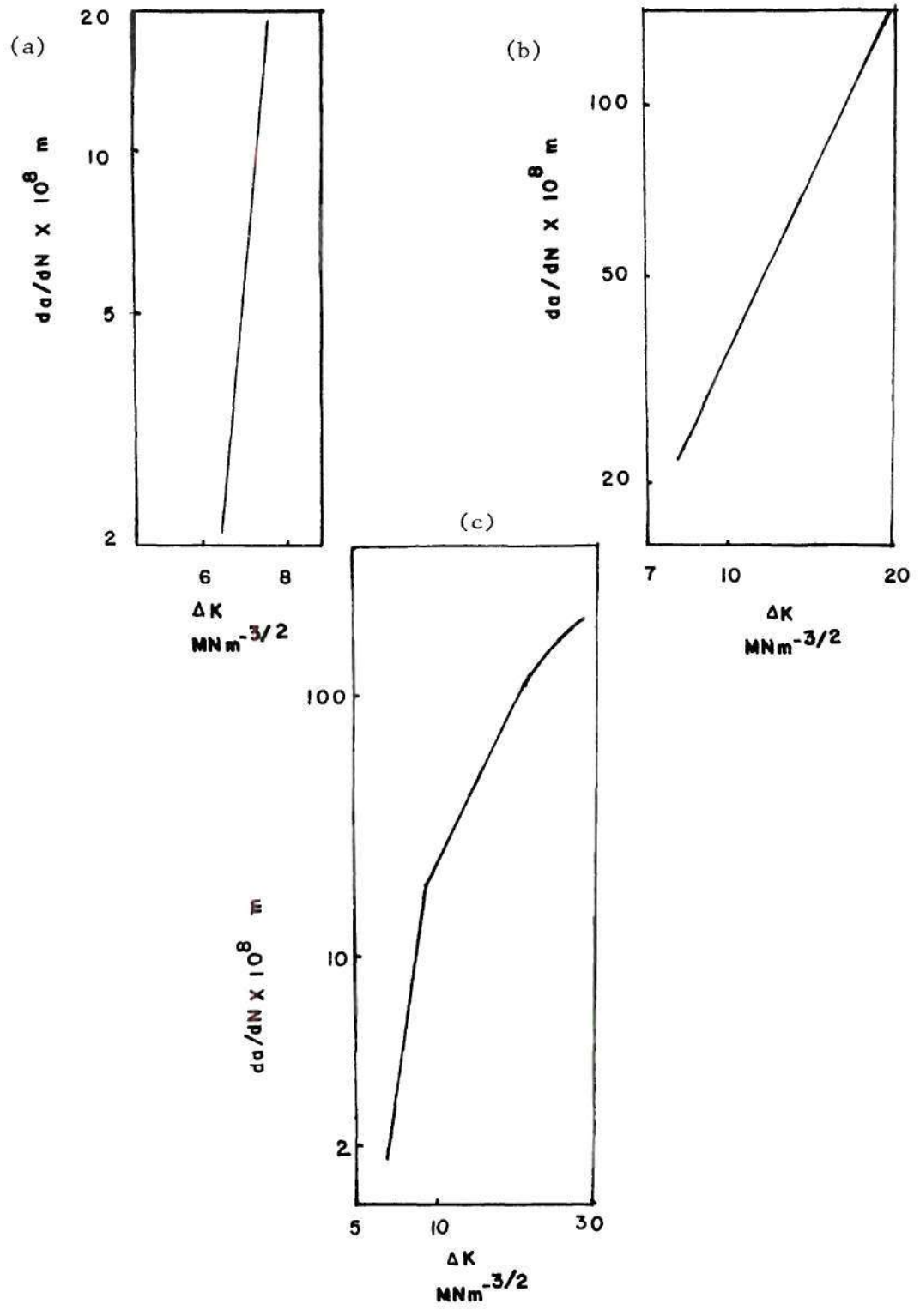

Figure 8. Fatigue Crack Growth Plots, da/dN vs. ΔK, for the Double Aged Condition: (a) low ΔK range, (b) intermediate ΔK range, and (c) entire crack growth plot.

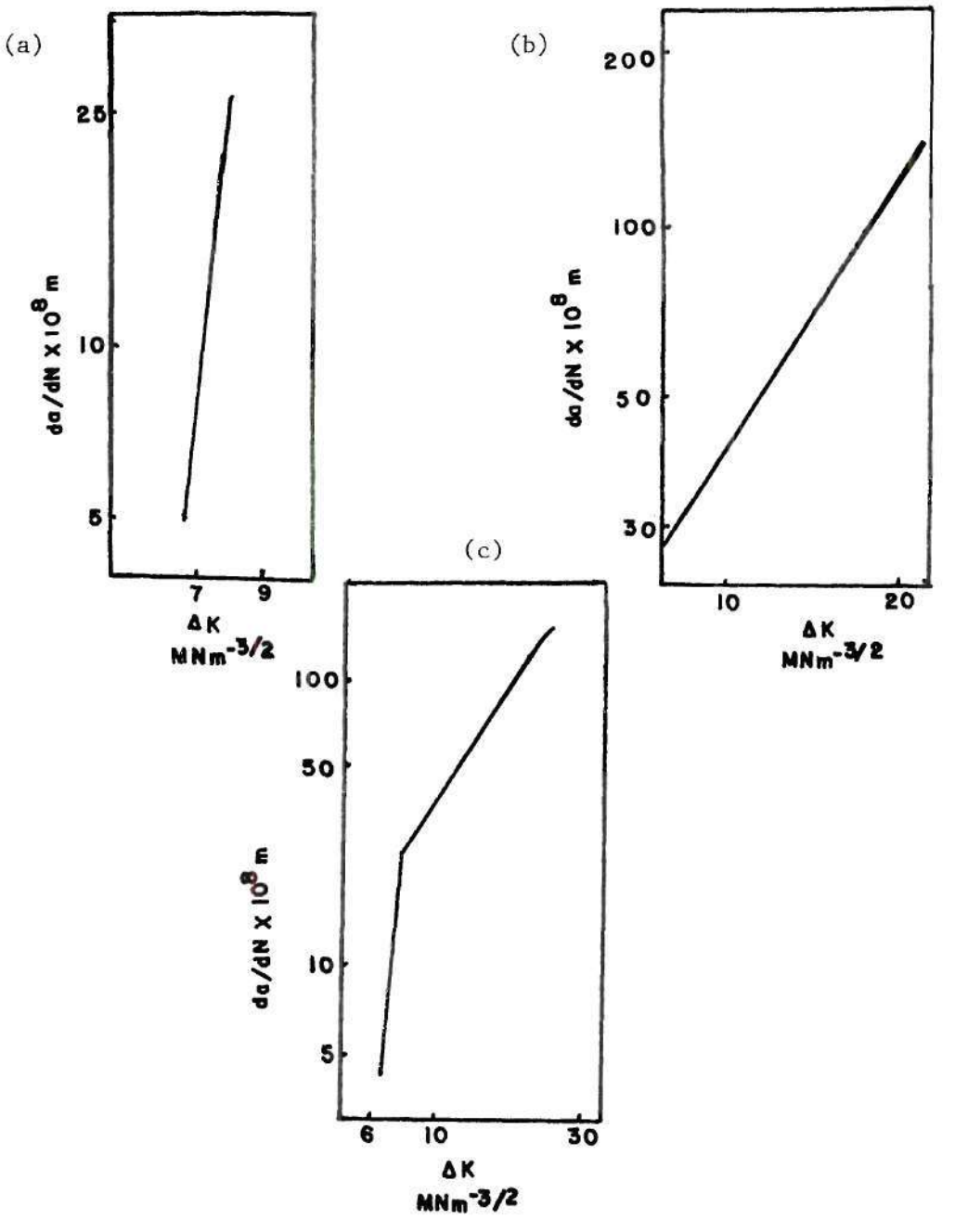

Figure 9. Fatigue Crack Growth Plots, da/dN vs. ΔK, for the Underaged Condition: (a) low ΔK range, (b) intermediate ΔK range, and (c) entire crack growth plot.

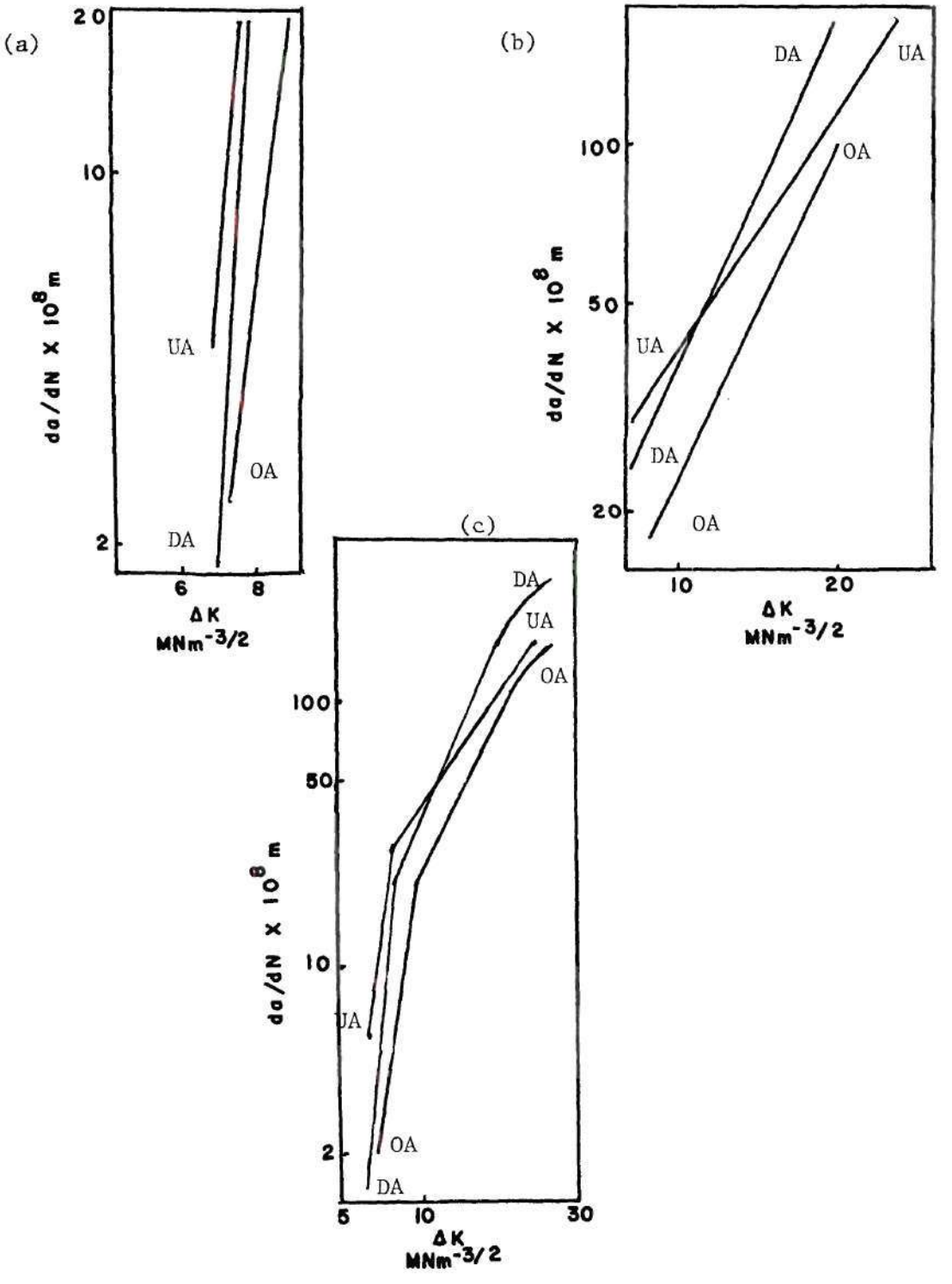

Figure 10. Superposition of the Fatigue Crack Growth Plots, da/dN vs. ΔK, for the Three Aging Conditions: (a) low ΔK range, (b) intermediate ΔK range, and (c) entire crack growth plot.

Table 4. Comparison of Crack Growth Rates

For Given Values of ΔK.

ΔK Level $MNm^{-3/2}$	Double Aged	Overaged	Underaged
	Crack Growth Rate X 10^{8} m		
6.5	2.7	*	*
8.0	22.5	6	27
9.5	33.5	20	36
11.0	46	27	46
12.5	62	36	56
14.0	80	46	66
15.5	100	57	77
17.0	125	70	88
18.5	155	84	100
20.0	**	98	114

* Not observed.

** ΔK exceeds linear portion of graph.

predicted by some of the proposed crack growth laws was attempted for the straight line portions, both low and intermediate ΔK values, of the da/dN vs. ΔK plots. In all cases some unknowns needed to be found. The Paris power equation was found to predict exactly for the straight line crack growth rates, once the values of the coefficient and exponent were found. These unknowns, as was the case with all the unknowns, were found by a computer program which took an initial guess for unknowns and worked towards values which gave the least error when compared to the observed results. The values for the Paris equation varied greatly according to the heat treatment and microstructure. A list of these parameters, as well as those determined for the other equations are presented in Table 5. The calculated growth rates using the Paris equation, as well as those calculated from the other equations, are presented in Appendix I.

The strain hardening models proposed by Head[31] and McClintock[32] failed to predict crack growth rates with an acceptable degree of accuracy. The model proposed by Head is based solely on monotonic parameters. This model predicted crack growth rates which were three orders of magnitude less than the observed values. McClintock's equation is based on monotonic parameters and the size of the plastic and process zone, i.e. the region in which the failure criterion is satisfied (see Figure 11). Correlation plots showing the observed and calculated growth rates using McClintock's formula are presented in Figures 12 and 13. Two sets of correlation graphs are presented. This formula has two values which were not precisely known, ε_y and ρ.

Table 5. Fatigue Crack Propagation Parameters

Aging Treatment and ΔK Range	Values for Paris Equation		Values for Antolovich Equation Using ε_f		Values for Antolovich Equation Using ε_f'	
	A	m	α	S	α	S
Double Aged Low ΔK	1.54E-16	10.23	2.45E15	10.01	1.87E16	10.01
Double Aged Int. ΔK	1.61E-09	2.36	1.70E-2	.26	1.44E-1	.29
Overaged Low ΔK	3.36E-14	6.93	9.09E05	5.27	1.74E07	5.06
Overaged Int. ΔK	1.38E-09	2.20	6.39E-2	.20	3.06E-2	.20
Underaged Low ΔK	1.12E-16	10.58	3.60E12	8.68	9.27E12	8.68
Underaged Int. ΔK	1.43E-08	1.45	1.30E-3	-.50	3.24E-3	-.50

Note: 1.54E-16 = 1.54×10^{-16}.

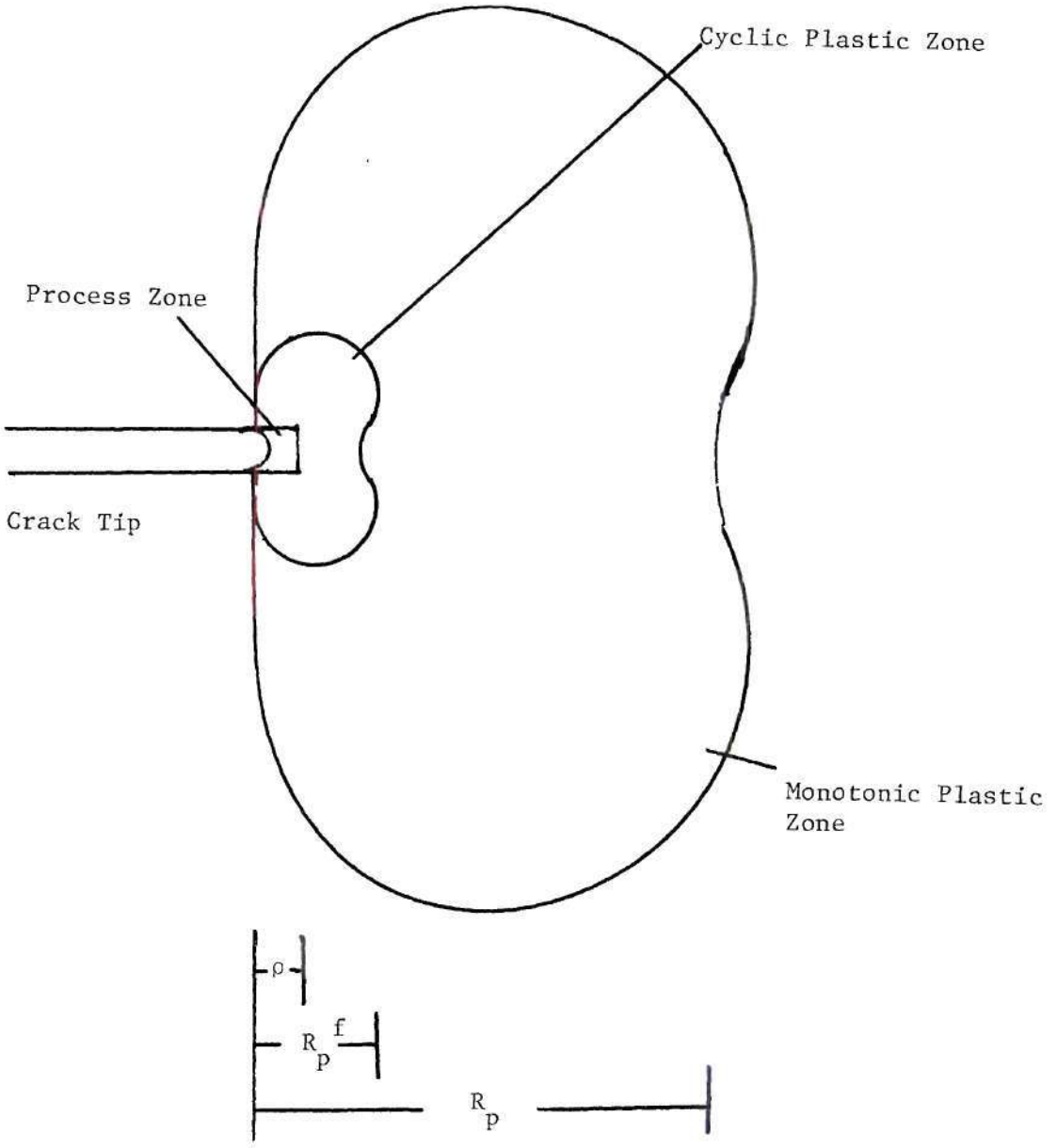

Figure 11. Schematic Showing the Process Zone and the Two Plastic Zones.

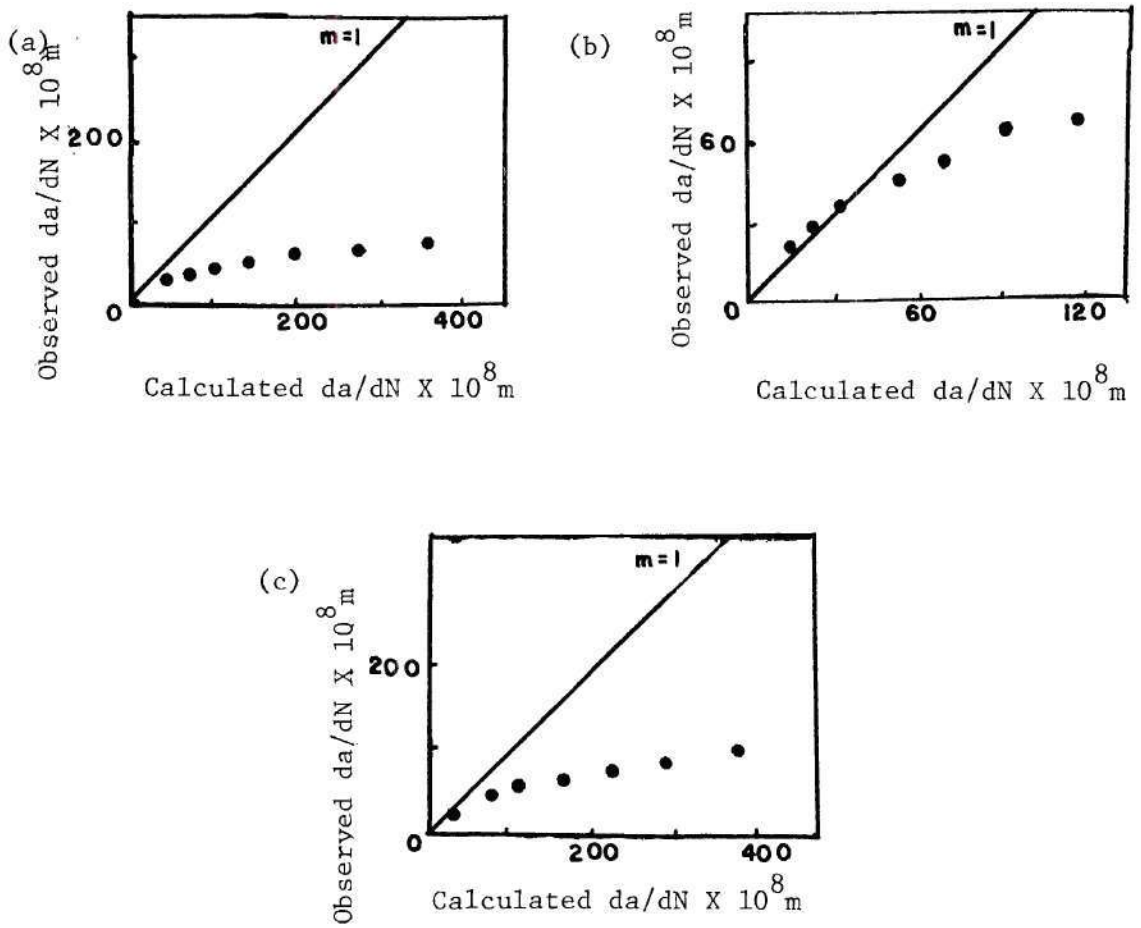

Figure 12. Comparison of the Predicted Crack Growth Rate and the Observed Rate Using the McClintock Equation with $\rho = 10^{-5}$m and Varying ε_y for the Intermediate ΔK Range: (a) underaged condition, (b) overaged condition, (c) double aged condition.

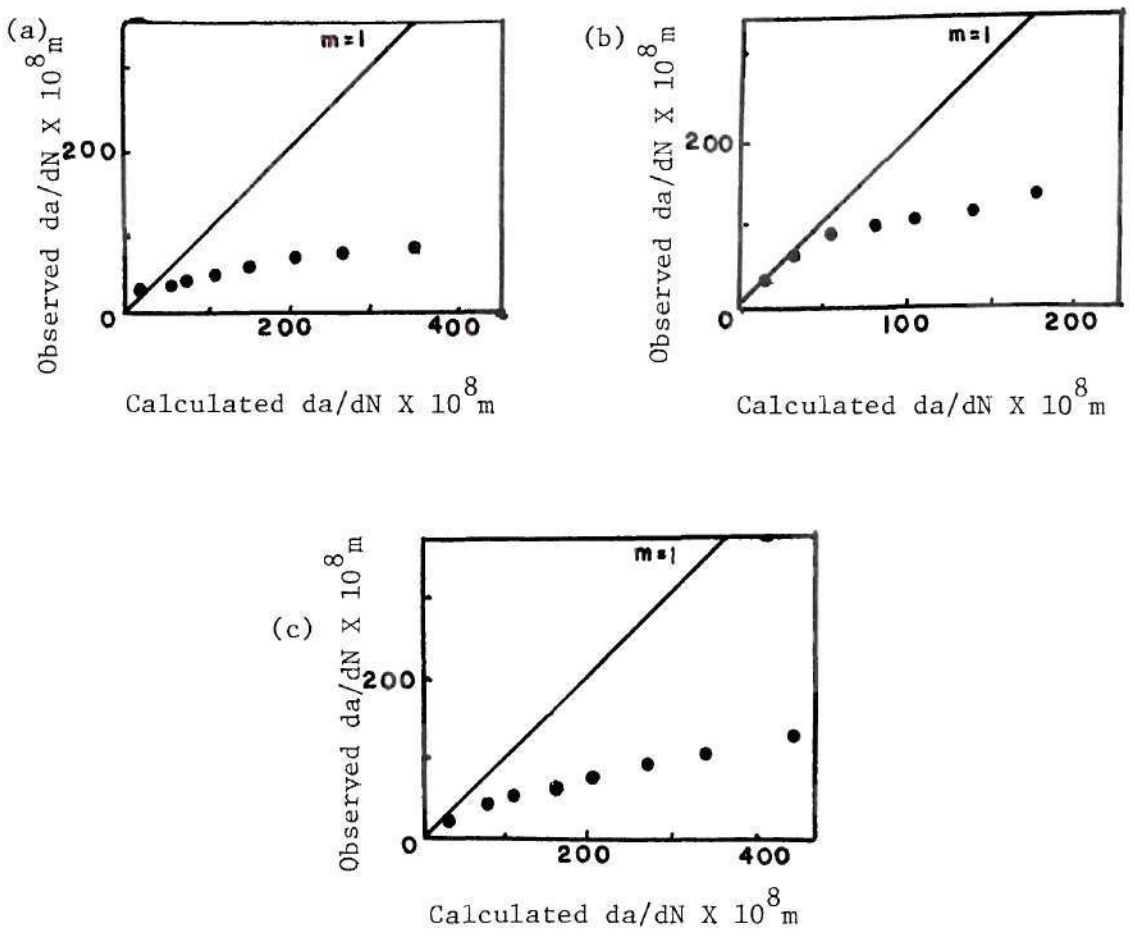

Figure 13. Comparison of the Predicted Crack Growth Rate and the Observed Rate Using the McClintock Equation with ε_y = the Strain at the Proportional Limit and ρ Varies for the Intermediate ΔK Range: (a) underaged condition, (b) overaged condition, and (c) double aged condition.

ε_y was estimated from previous tensile work[6] and values for ρ were assumed to be near the values of ρ, within an order of magnitude, found by Selines[2] for 7075. The graphs presented in Figure 12 were obtained by varying ε_y until growth rates similar to the observed ones were found, while Figure 13 is for values of ρ being varied until the right growth range was found. Altering both values did not produce results which were closer to the observed results than those shown in Figures 12 and 13.

Monotonic and low cycle fatigue parameters are used in the crack growth expression proposed by Antolovich[37]. This equation predicts the crack rates with a high degree of accuracy, once the correct values for α and S are known for the particular aging treatment. Figures 14 through 16 show plots of the observed crack growth rates and the calculated rates for the Antolovich equation, using the calculated values of α and S. The values of α and S were also calculated using the vlaue of ε_f', the fatigue ductility coefficient.

Scanning electron micrographs of the fracture surfaces for each aging treatment are shown in Figures 17 through 19. Fatigue striations were not observed on the specimens tested at low ΔK values, but were observed on those tested at intermediate ΔK values for the aging treatments tested. For local crack growth, i.e. across a single grain, the striations were observed to deviate from the direction parallel to the direction of the gross crack growth. Small intergranular cracks were observed on the fracture surfaces for most ΔK values. These cracks were present on specimens of each aging

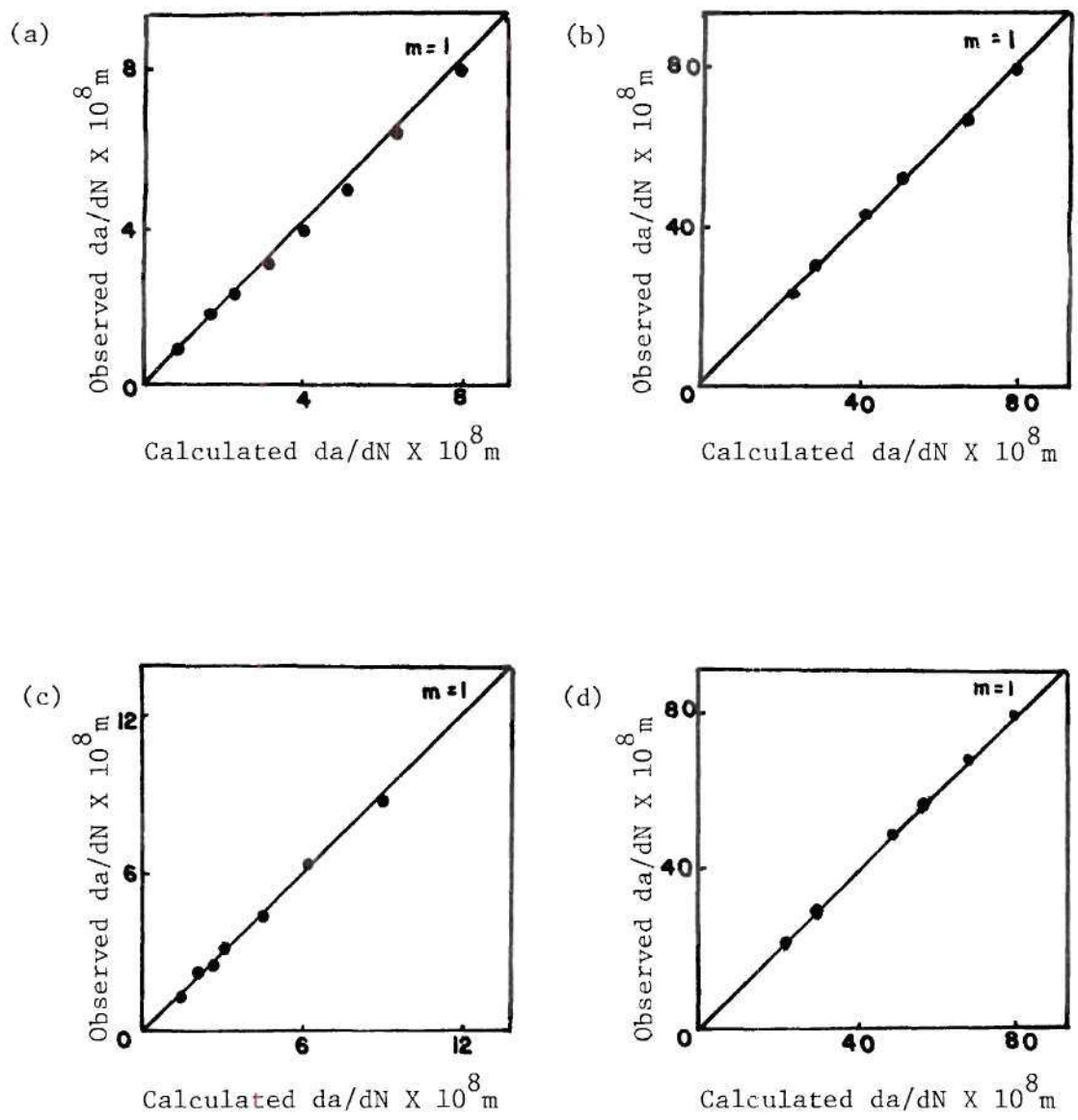

Figure 14. Comparison of the Predicted Crack Growth Rate and the Observed Rate Using the Antolovich Equation: (a) low ΔK range using ε_f, (b) intermediate ΔK range using ε_f, (c) low ΔK range using ε_f', and (d) intermediate ΔK range using ε_f'. Double Aged Condition.

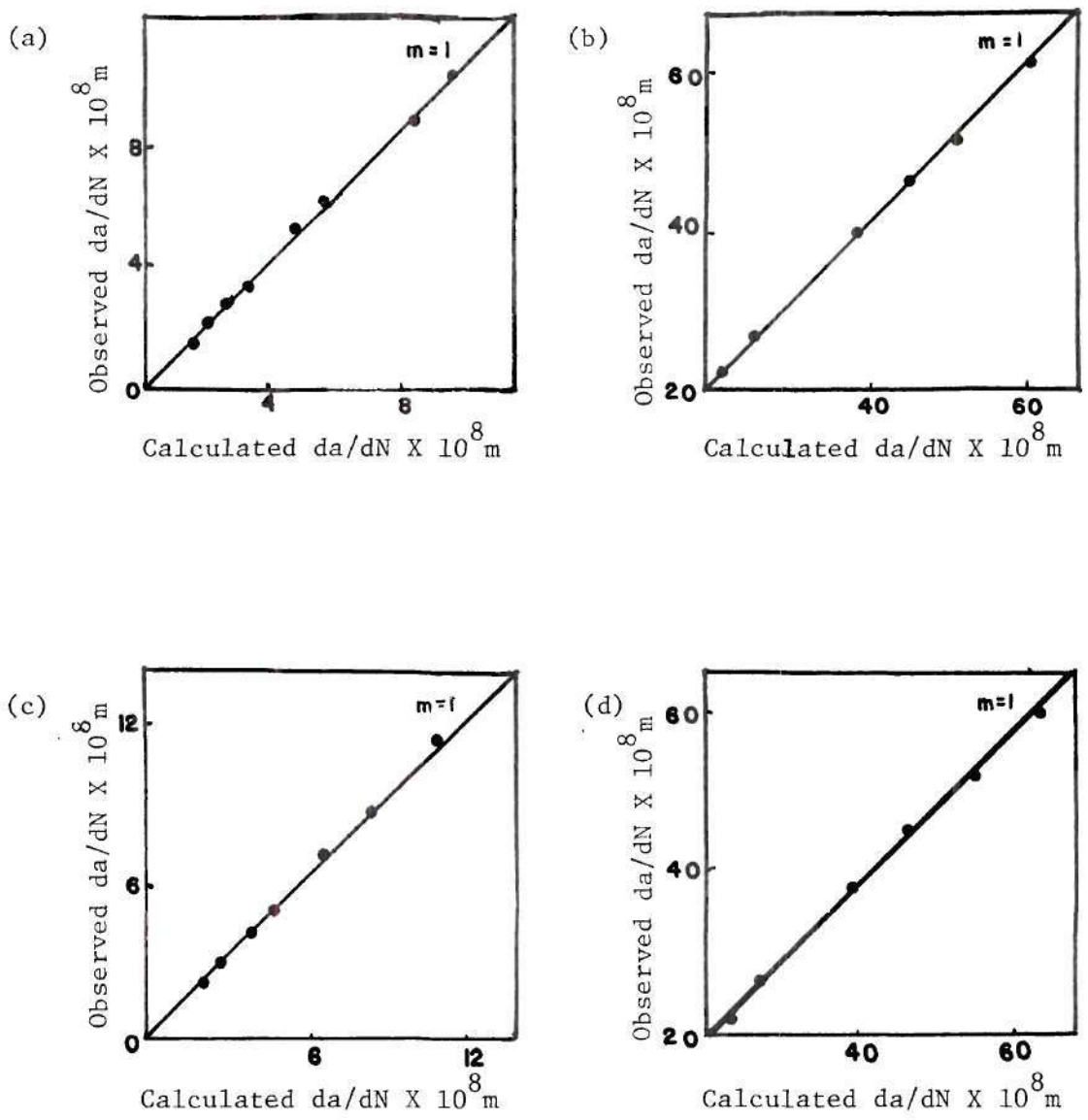

Figure 15. Comparison of the Predicted Crack Growth Rate and the Observed Rate Using the Antolovich Equation: (a) low ΔK range using ε_f, (b) intermediate ΔK range using ε_f, (c) low ΔK range using ε_f', and (d) intermediate ΔK range using ε_f'. Overaged Condition.

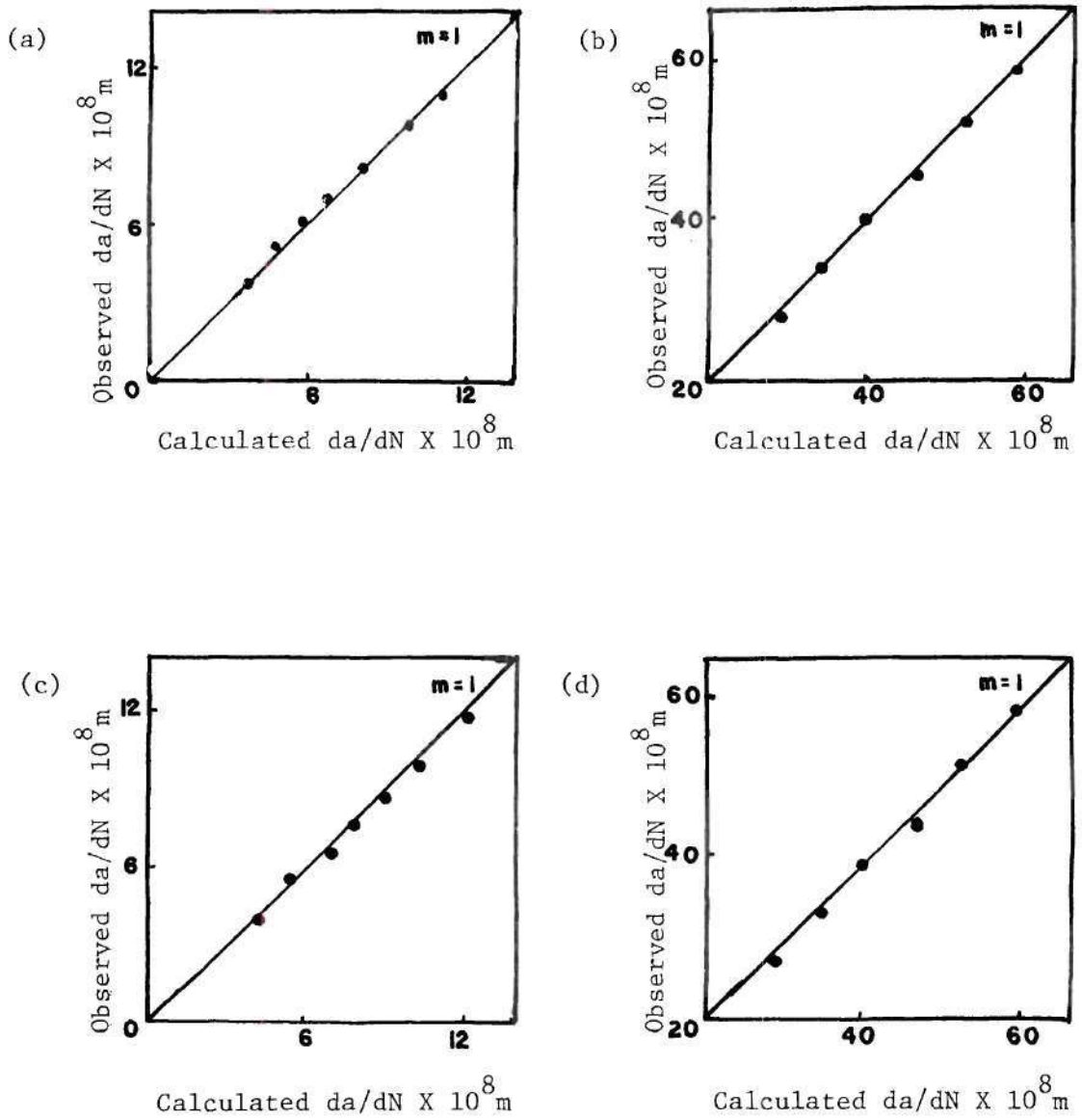

Figure 16. Comparison of the Predicted Crack Growth Rate and the Observed Rate Using the Antolovich Equation: (a) low ΔK range using ε_f, (b) intermediate ΔK range using ε_f, (c) low ΔK range using ε_f', and (d) intermediate ΔK range using ε_f'. Underaged Condition.

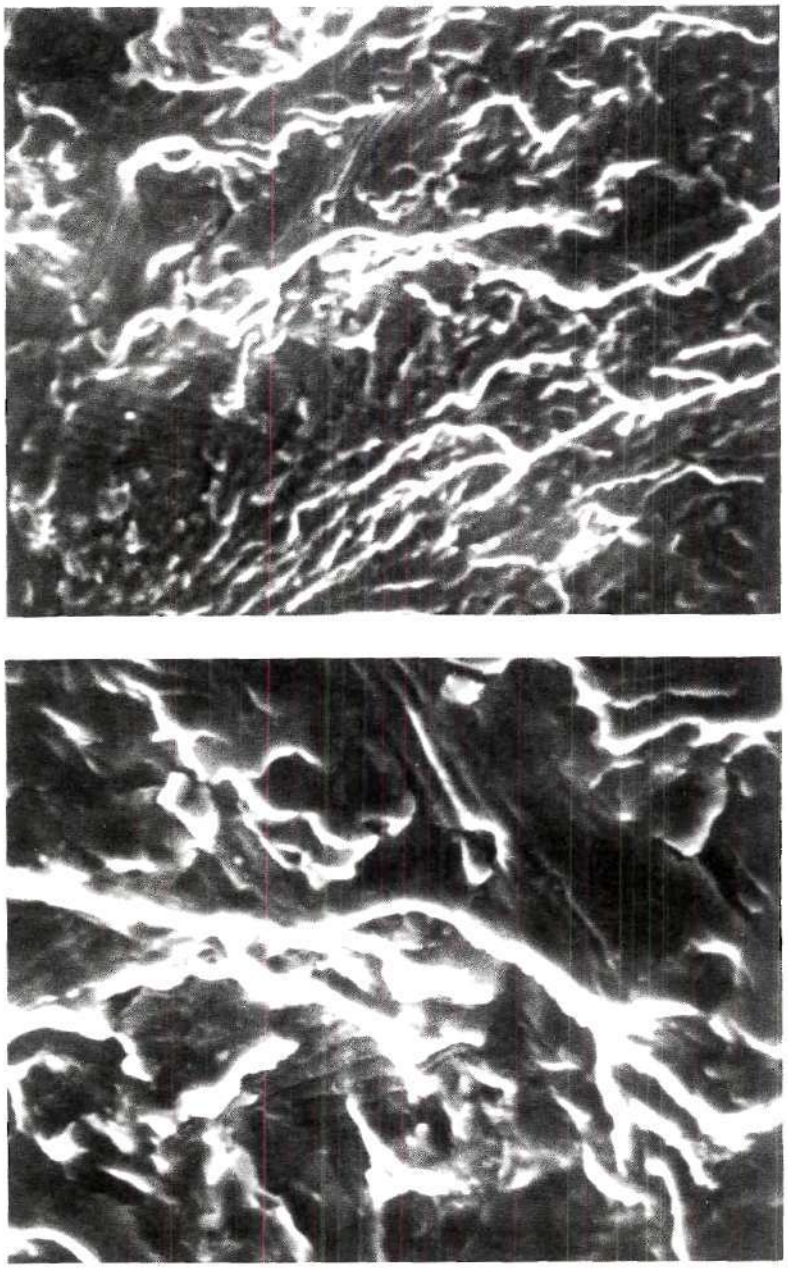

Figure 17. Typical Scanning Electron Micrographs Showing General Features of the Double Aged Condition.

Crack direction

500X

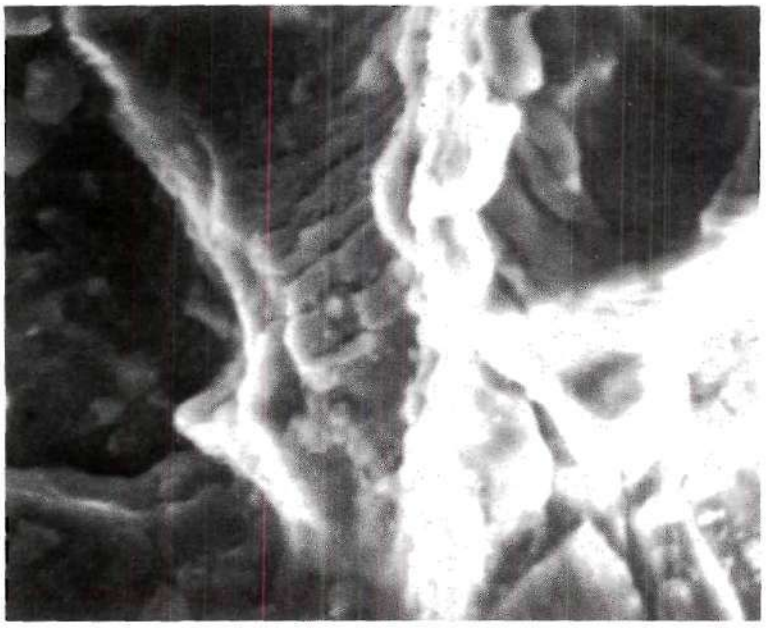

Crack direction

3500X

Figure 18. Typical Scanning Electron Micrographs Showing General Features of the Overaged Condition.

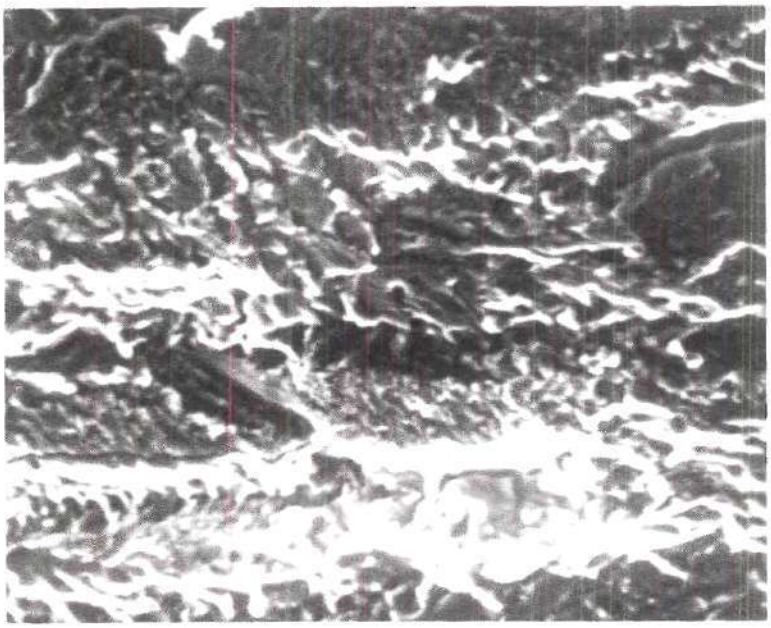

Crack direction

500X

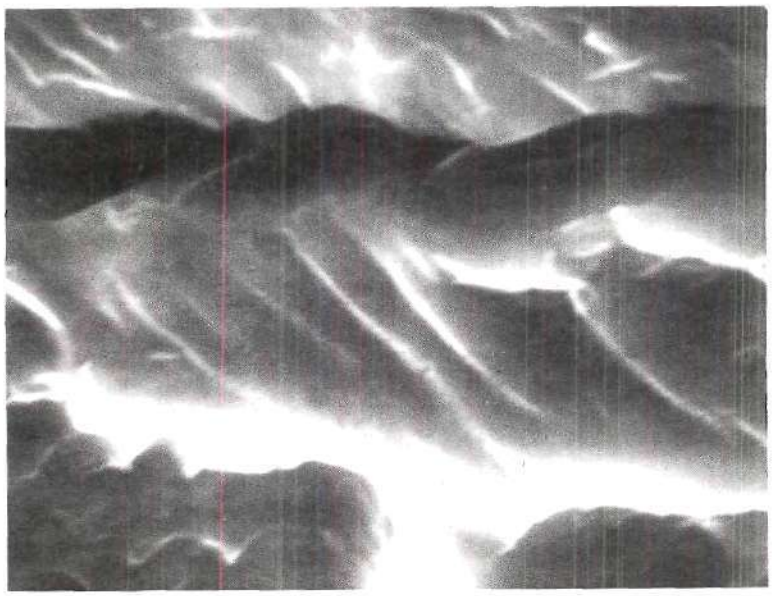

Crack direction

8600X

Figure 19. Typical Scanning Electron Micrograph Showing General Features of the Underaged Condition.

treatment, but were more prevalent on surfaces of the underaged condition. A combination of intergranular and transgranular fracture was present for all aging conditions. The double aged condition exhibited the least degree of intergranular growth and the underaged exhibited the highest degree. The inclusions were observed to have very little effect on the striation spacing.

CHAPTER V

DISCUSSION OF RESULTS

The results show that there is not a direct relationship between monotonic strength parameters and fatigue crack growth rates. The monotonic yield strengths for the underaged and double aged treatments were 20% different, 368 MNm^{-2} and 445 MNm^{-2} respectively, but the crack growth rates were not really different. On the other hand, the underaged and overaged treatments produced similar yield strengths, 368 and 378 MNm^{-2} respectively, but the growth rates, at least for low ΔK values, were different. This agrees with the findings at Alcoa[3] that there is not a correlation between monotonic yield strength and crack growth rates for 7XXX alloys. Likewise the monotonic yield strain seems to have no correlation with the crack growth rate. The ultimate tensile strengths of the three aging treatments vary a total of 12%, 412 to 469 MNm^{-2}. The order in which the ultimate strengths increase, i.e. overaged, underaged and double aged does not correspond, directly or inversely, to the crack rates at low ΔK values. Between ΔK values of 10 and 15 MNm^{-2} the relative crack growth rates varied inversely with the relative ultimate strengths. This correlation is, however, probably coincidental since the underaged treatment appears as though it would have a slower crack growth rates at ΔK values higher than those used in the tests. This is in agreement with Selines[2] conclusion

that a low strain monotonic work hardening coefficient, uniform reduction in area and the degree of cyclic hardening are all measures of the materials ability to resist localized deformation.

The low cycle fatigue ductility coefficient, ε_f', appears to be the low cycle fatigue parameter which best indicates the relative crack growth rates, at low ΔKs, during FCP, for the aging treatments tested. The larger the value of ε_f' the smaller the crack growth rate for a given ΔK value. The values of ε_f' at low ΔKs, for the underaged and double aged treatments were similar to each other, 43% and 98% respectively when compared with the value for the overaged condition, 632%. A change in slope was observed in the Coffin-Manson plot for the overaged conditions. At the higher strain values an ε_f' value of 48% was observed. This value is similar to the ε_f' values of the other aging conditions. The growth rates for the three conditions are also similar in the higher strain, or intermediate ΔK, region. The ε_f' values give an accurate ranking of the crack growth rates at both the low and intermediate ΔK ranges for the alloy and aging conditions tested. The closeness of the ε_f' vlaues for the underaged and double aged treatment is similar to the closeness of the crack growth rates whereas the larger value of ε_f' for the overaged condition relates to the decrease in crack growth rates. The relative rankings of the Coffin-Manson exponent, -C, and the cyclic work hardening exponent, n', are the same as that of the fatigue ductility coefficient. This agrees with the suggestion of Feltner and Beardmore[45] that an increase in n' will lead to an increased resistance to cyclic plastic strains which would lead to an

increase in fatigue life and a decrease in crack growth rates.

Since all FCP samples received the same homogenization treatment and had constant grain sizes whatever microstructural effects are present must be due to the precipitate type and size. The precipitate sizes for the 4 hours at 120°C and the double aging treatment were approximately the same, as were the growth rates, although the precipitate types were different. The precipitate type for the overaged condition was similar to that of the double aged samples but the sizes varied by a factor of 2.5. The precipitate spacing, assuming a constant volume fraction of precipitates, for the overaged condition is 1.6 times the spacing of precipitates in the double aged condition. The larger spacing in the overaged condition would permit a larger degree of cross slip which would reduce the reversibility of slip. The improved fatigue life of the overaged condition was attributed to increased homogeneity of slip resulting from the occurrence of dislocation looping as the primary deformation mechanism. Thus it appears that at low ΔKs the precipitate size or spacing is a more important factor in determining fatigue crack growth rates than is precipitate type. The larger precipitates, with a lower density, appears to be the preferred microstructure when the minimum crack growth rate is desired. This corresponds to previous work done by Thompson et al[26]. As the ΔK range is increased, the underaged conditon begins to show lower crack growth rates than the double aged condition and the growth rates begin to approach the lower rates observed for the overaged condition. This observation

appears to support the work of Kershaw[25] which found that the effect of the particles is dependent on the stress intensity range and that the effect decreases as the ΔK range is increased.

At low ΔK values a real crack growth rate difference is observed between the different microstructures, which can be due to the differences in the homogeneity of deformation. The overaged condition, which has the slowest crack velocity at a given ΔK level, exhibits the largest degree of homogeneous deformation due to the dislocation looping of incoherent particles[44]. The underaged and double aged conditions exhibit dislocation banding, resulting in inhomogeneity of deformation[43]. As the ΔK level is increased, and hence the strain is increased, evidence of dislocation banding disappears[44], resulting in a smaller difference in the homogeneity of deformation. This smaller difference may explain the smaller differences in observed crack rates at the intermediate ΔK level. The growth rates at the intermediate ΔK level were within a factor of 2 for all these conditions, which could be within experimental error. Hence the effect of constituent particles at low ΔK levels is to change the degree of homogeneity of deformation and thus alter the growth rate, but as the ΔK level increases the effect of the particles becomes smaller. The observed lack of influence of constituent particles at intermediate ΔK levels agrees with work done at Alcoa[3].

The homogeneity of deformation differs in the three microstructures. The overaged condition, with a microstructure of large η particles, exhibited the smallest crack growth rates at a given ΔK value in the

low ΔK ranges. A greater incidence of dislocation looping appears in this aging treatment which results in a more homogeneous deformation[44]. This same aging treatment was found to produce the best low cycle fatigue resistance. Selines[2] proposed that the fatigue crack growth resistance in the low ΔK region is directly related to the materials ability to distribute small, cyclic plastic strain amplitudes homogeneously and to avoid localized areas of high strain concentration. Grosskreutz and Shaw[46] found that the production of large Mn rich particles into 2024 by overaging increased the overall fatigue life for axial S-N tests by promoting a wavy slip mode and a homogeneous dislocation distribution. The large, incoherent η particles, which promote dislocation looping rather than particle shearing, cause a more homogeneous mode of deformation, resulting in slower crack rates at low ΔK values.

The crack path in the double aged alloy was observed to follow an intergranular path whenever possible. For the other aging treatments the cracks were found to propagate in a straighter line, regardless of whether the crack travelled intergranularly or transgranularly. This fact agrees with the dependence of the crack path on aging conditions found by Nageswararao et al[4]. They found that, in high purity Al-Zn-Mg alloys, the material aged to maximum hardness and tested in a moist environment showed a greater percentage of intergranular fracture than for any other combination of factors.

The underaged specimens exhibited frequent, macroscopic crack branching. The net effect of the crack branching is to disperse the

strain field energy among multiple crack fronts, increase the surface area being generated and hence slow down the macroscopic crack growth. The crack branches tend to have a definite angular relationship with the propagating crack, indicating that the crack grows along certain crystallographic orientations and that only certain favorable oriented directions permit branching. The branched crack grows at a much slower rate than it did prior to branching, see Table 6. Severe slip markings have been observed on tensile samples in the underaged condition[44]. The dislocations shear the G.P. zones resulting in planar slip and tend to remain on a single glide plane and cross slip becomes difficult. As the dislocations multiply and become entangled on the glide planes slip reversibility becomes difficult resulting in the development of notch-peak topography.

The scanning electron micrographs failed to show fatigue striations at low values of ΔK, Figure 20. The lack of observed striations may be due to the poor resolution of scanning electron microscopy or to the fact that aluminum is a light metal and thus scatters a large number of electrons. Striations may be visible if replicas were made of the fracture surface or if the surface was plated with a heavier metal, e.g. gold. In lieu of striations the surface could be characterized as consisting of plateaus and ridges and some rumpled areas, using the nomenclature of Weber and Hertzberg[47]. This type of fracture surface is shown in Figure 20 (a). The fracture surfaces observed for low ΔKs were much flatter than those created at intermediate ΔK values, Figure 21. No difference was observed on the fracture surfaces for the various aging treatments in the low ΔK

Table 6. Comparison of Crack Growth Rates for Single Cracks and Branched Cracks for the Underaged Condition

ΔK $MNm^{-3/2}$	$da/dN \times 10^{8}$ m single crack	$da/dN \times 10^{8}$ m branched crack*
7.75	25	1.5
7.90	26	1.2
8.00	27.5	1.2
8.20	30	.7-1.5
8.40	31	.7-2.0
8.60	32	2.9
8.80	33	2.7
9.0	34	2.75
10.0	40	15.0
12.0	53	27.0
14.0	66	21.0

* More than one additional branch may form during testing; range represents observed range on several samples, the number of extra cracks varies.

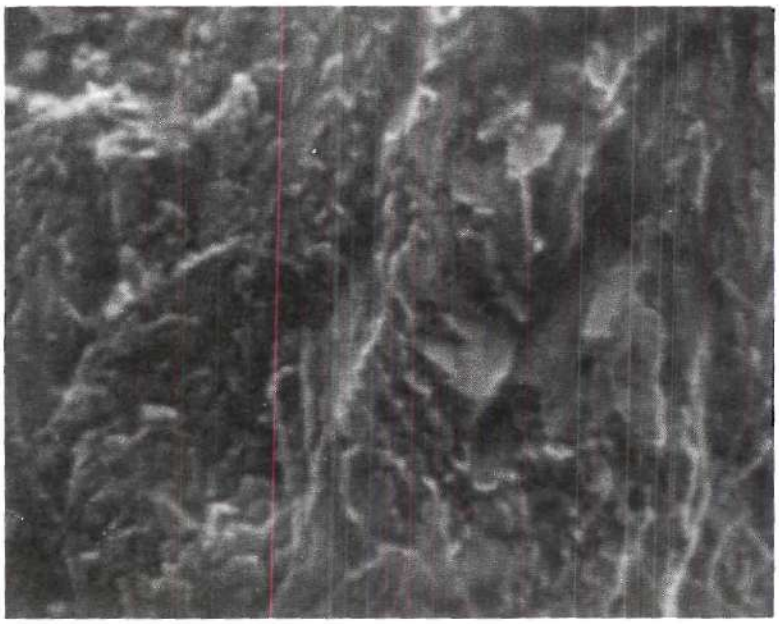

(a)

Crack direction

750X

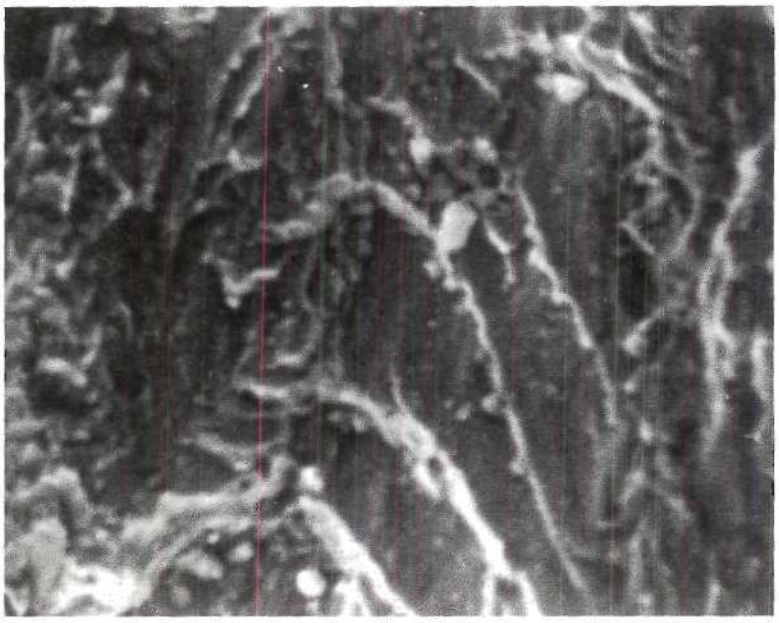

(b)

Crack direction

750X

Figure 20. Scanning Electron Micrographs of Fracture Surfaces Formed at a Low ΔK Value on Overaged Specimens: (a) plateaus and ridges, (b) general features.

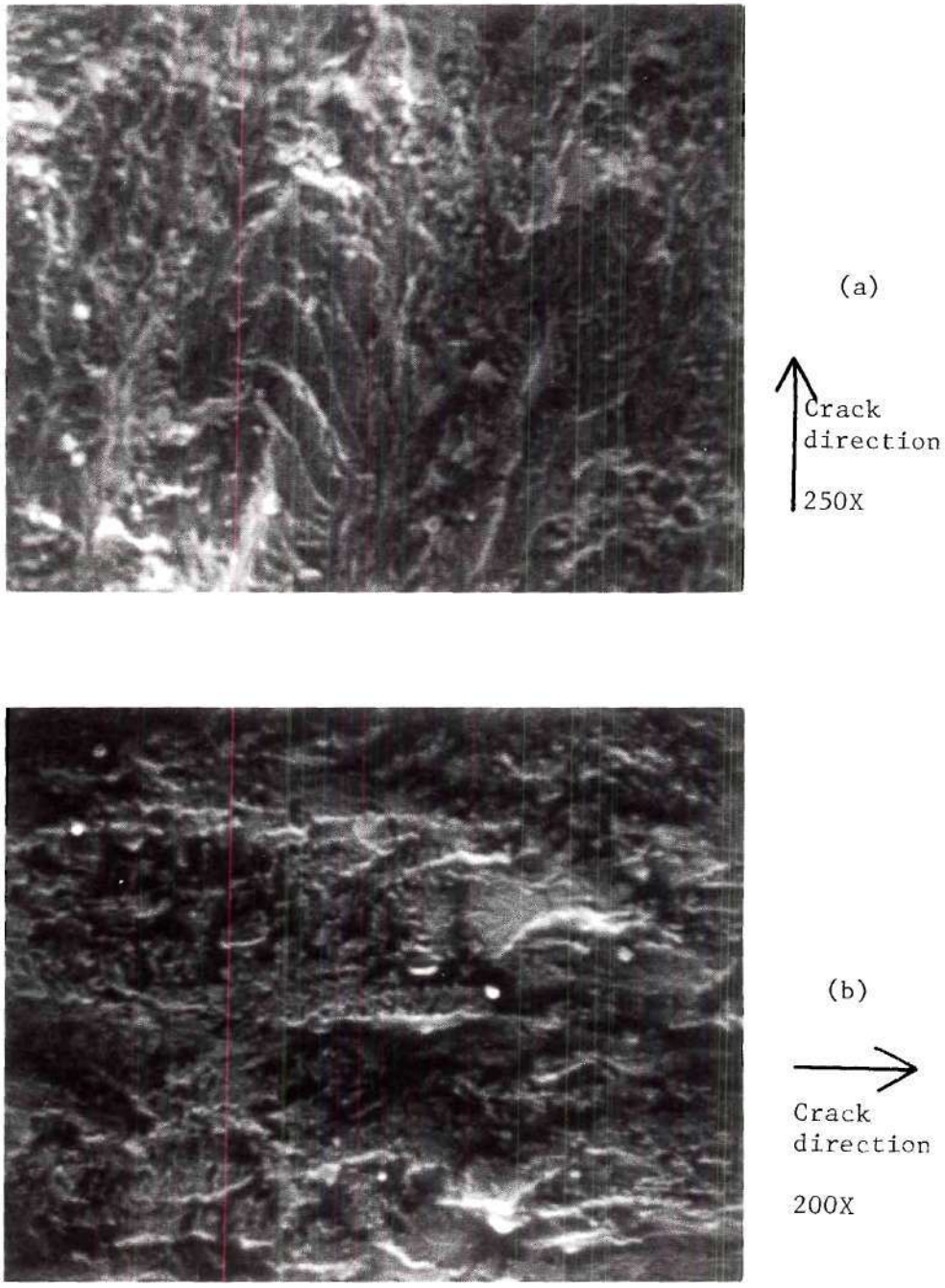

Figure 21. Scanning Electron Micrographs of General Fracture Surfaces Formed at an Intermediate ΔK Level: (a) overaged condition, and (b) underaged condition.

regions.

In the intermediate ΔK range the fatigue striations are sharp and readily visible for the double aged condition, Figure 22, while not as visible for the overaged condition, Figure 23. Researchers at Alcoa[3] have found the lack of visibility of striations in the maximum aged condition, T31, in 2XXX alloys, and sharp striations in the overaged condition, T86. Particles have little effect on the advancing crack front[3] as is shown in Figure 24. The striations show that the advancing crack was not interrupted by the particle which was removed by the other half of the crack surface. Figure 25 shows the local variation in the direction of the crack. The crack appears to grow in a preferred direction across the individual grains, possibly along a preferred crystallographic slip direction.

The superposition of the da/dN vs. ΔK graphs, Figure 10, shows that the differences in the crack growth rates for the different microstructures is small. The growth rates for the samples containing small, coherent GP zones, i.e. those aged 4 hours at 120°C, and the rates for the samples containing some small η, but mostly η' particles, i.e. those aged 2 hours at 120°C and 12 hours at 150°C, show virtually no difference over the range of ΔKs tested. The aging treatment of 24 hours at 150°C, producing large, incoherent η particles, produced a structure which consistently had a slower crack growth rate for a given ΔK.

The inhomogeneous deformation associated with age-hardenable aluminum alloys makes the testing of any theoretical model of fatigue crack growth difficult at least. The Paris equation can be made to

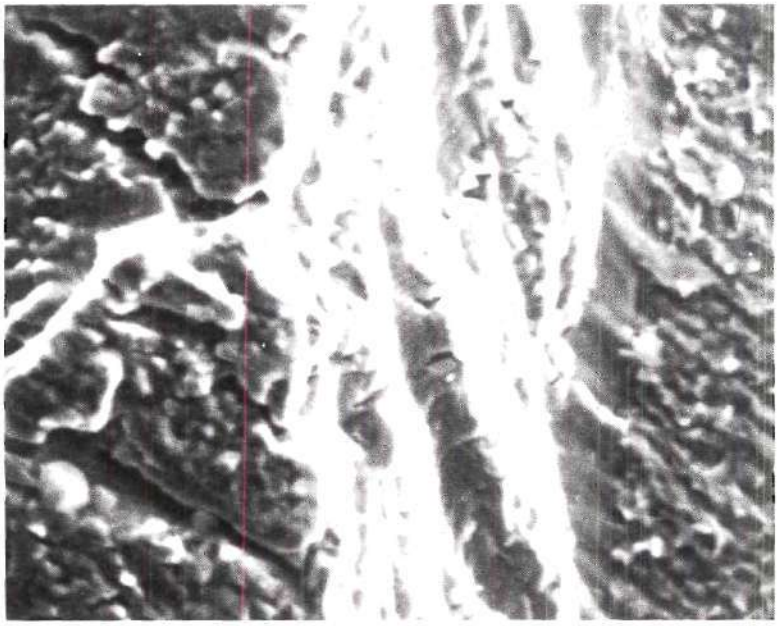

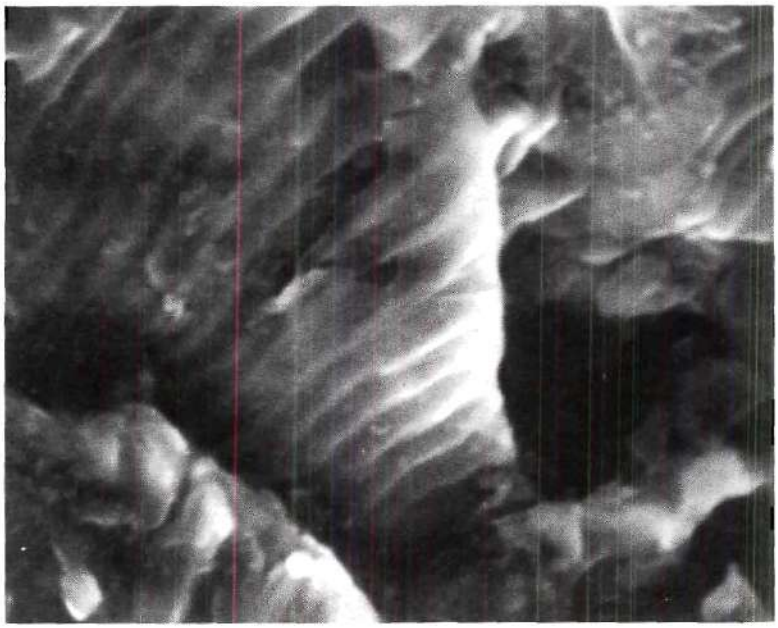

Figure 22. Scanning Electron Micrographs Showing Sharp and Readily Visible Fatigue Striations for the Double Aged Condition.

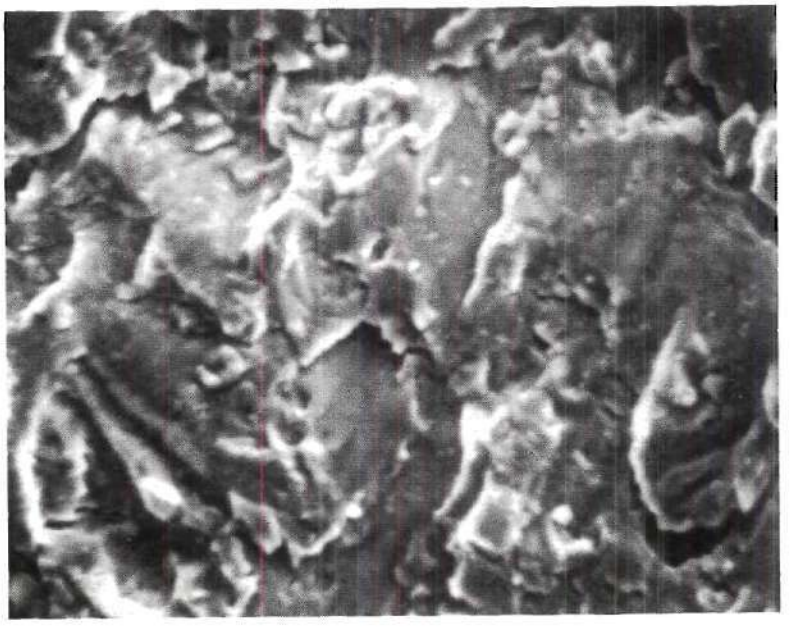

Crack direction

500X

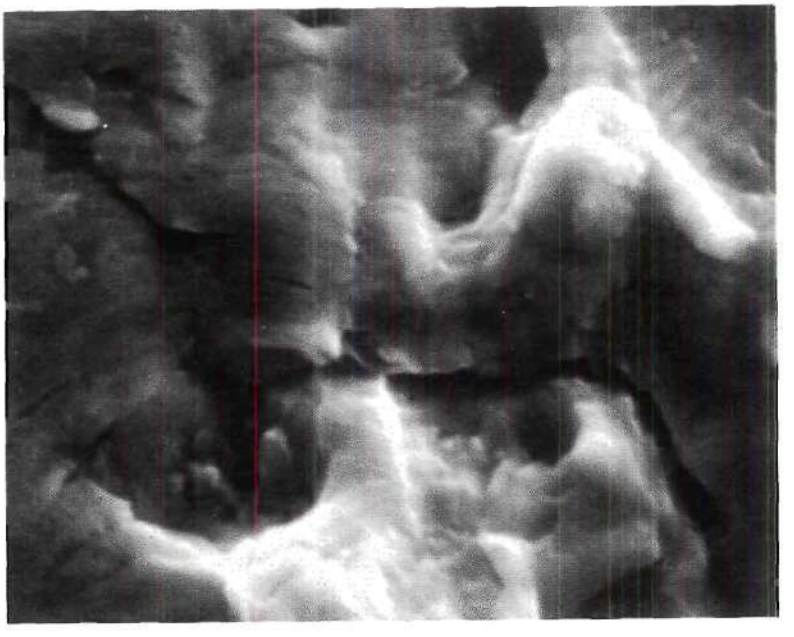

Crack direction

4200X

Figure 23. Scanning Electron Micrographs Showing the Lack of Clearly Visible Fatigue Striations for the Overaged Condition.

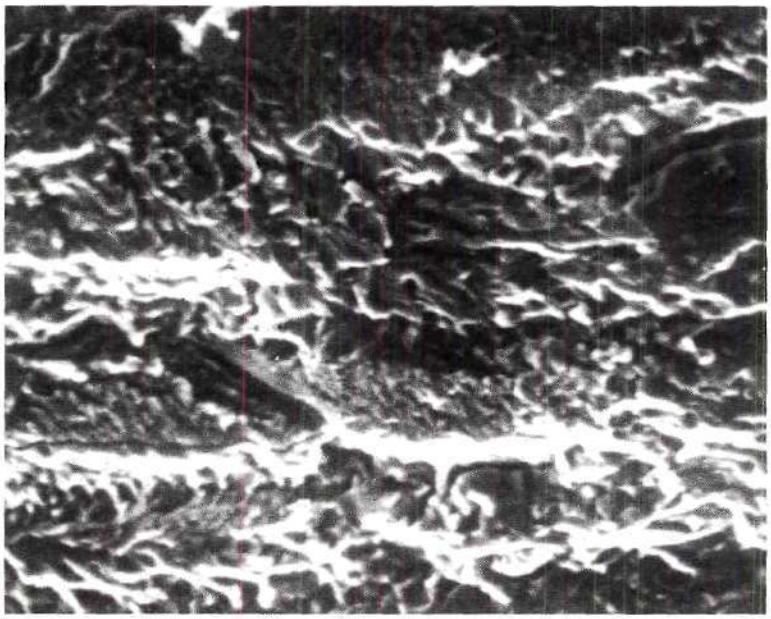

(a)

Crack direction

500X

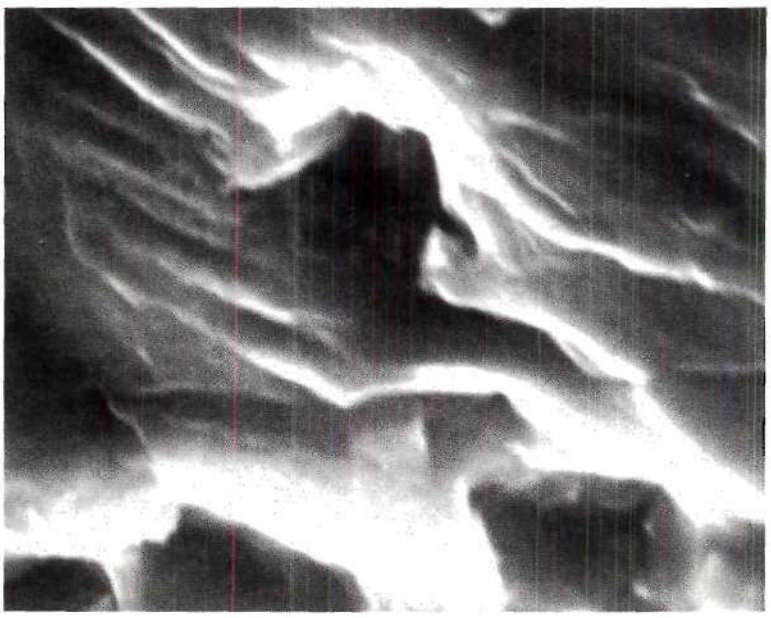

(b)

Crack direction

8600X

Figure 24. Scanning Electron Micrographs Showing the Effect of Particles in the Advancing Crack Front: (a) underaged condition, and (b) underaged condition.

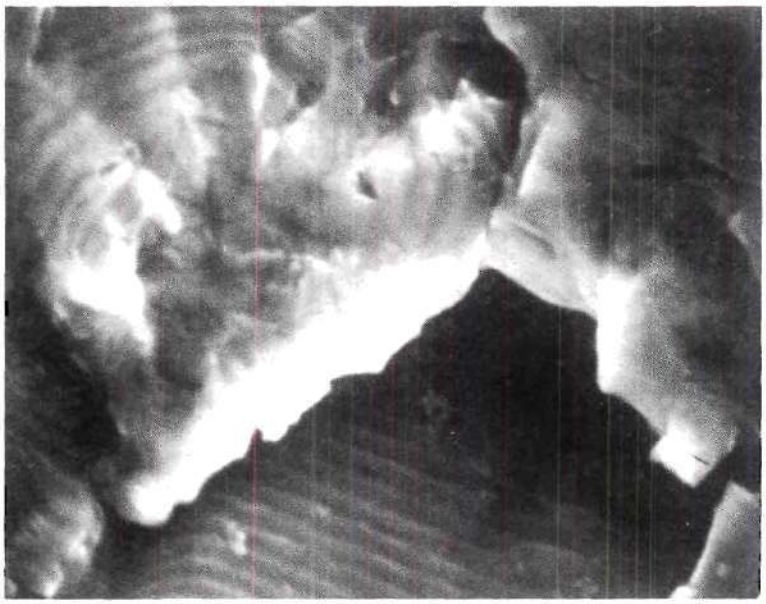

(a)

Crack direction

5000X

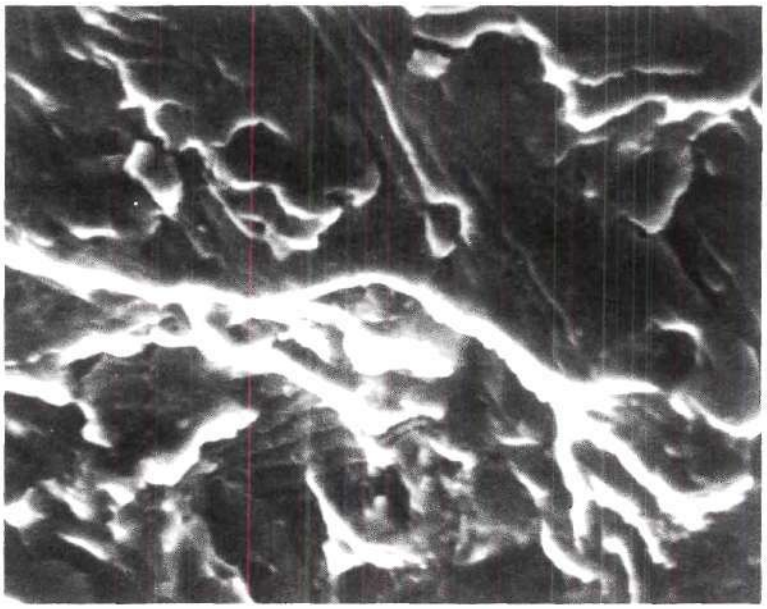

(b)

Crack direction

1750X

Figure 25. Scanning Electron Micrographs Showing the Local Variation in the Direction of the Crack: (a) overaged condition, and (b) double aged condition.

fit any data which produces a straight line on a log-log graph. The values of A and m varied for each aging treatment, as can be seen in Table 5. For the low ΔK region, which is usually not treated with the power law, the values of A and m were very similar for the underaged and double aged specimens, as was the observed crack growth rates. The value of A for the overaged condition was greater than for the other conditions, indicating that the da/dN vs. ΔK plots would cross one another at a sufficiently low ΔK. Such a ΔK value was below the range tested and probably below the threshold value of K to produce fatigue crack growth. The value for m was considerably smaller for the overaged condition than for the others. This allows the da/dN vs. ΔK plots to deviate as ΔK increases. For the intermediate ΔK range the values of m are similar for the double aged and overaged condition, indicating that the increases in crack rate with increasing ΔK levels would be similar. The values of m in this ΔK range are close to 2, the value generally accepted in most growth rate equations using the Paris equation as a basis. The value of A was different for the two conditions, the one for the overaged condition being smaller. This would indicate that the growth rate for the overaged condition would be less than that of the double aged condition for a given value of ΔK. While this difference appears to be real it is so small that differences in crack rates observed could be within experimental error. The values of A and m for the intermediate ΔK range and the underaged condition indicate that the crack growth rate for a given ΔK would be lower than that for the other conditions at some higher ΔKs than were used in the tests.

Further work would be needed to verify this result. A plot of log A vs. m is shown in Figure 26 to show the relationship between A and m for both the (a) low ΔK ranges and (b) the intermediate ΔK ranges.

Head[31] proposed a fatigue crack growth rate based on measured properties alone. His equation predicts the lowest crack growth rates for the underaged condition and similar rates for the other two conditions. The predicted rates are lower, by two orders of magnitude, than those observed in the low ΔK regime and three orders lower than those observed in the intermediate range. The value of the exponent for σ is two, and not a variable.

The work hardening model proposed by McClintock[32] was tested over the intermediate range only since it had a fixed power for the stress intensity level, i.e. 4. The Paris equation had predicted that a power value of 6 to 10 was necessary for the equation to accurately predict the proper growth rate. The cyclic parameter, ε_f', was substituted for the monotonic parameter, ε_f', since fatigue crack propagation is a cyclic process and the predicted crack growth rate was too high where ε_f was used. The two variable parameters, ρ and ε_y' the process zone size and yield strain, were originally picked to be near the values determined by Selines[2] for ρ and the proportional limit from tensile tests of alloy 7050. As can be seen from Figures 12 and 13 this particular growth law varies the growth rate too rapidly. This is caused by the fourth power dependence of K.

Antolovich[43] used the value of fracture strain, ε_f' in his equation predicting crack rates. Both the cyclic value, ε_f',

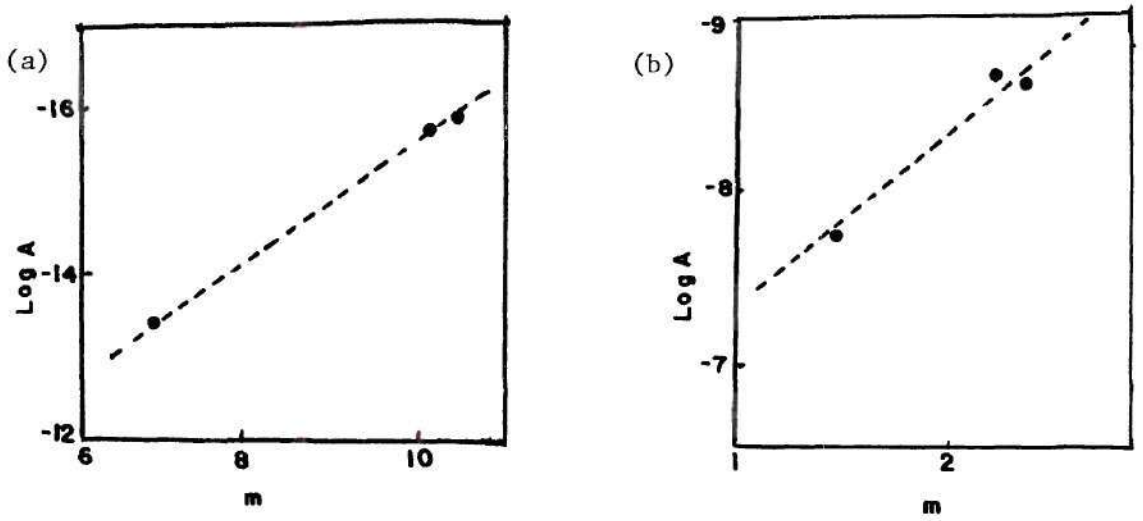

Figure 26. Relationship Between the Parameters A and m of the Paris Equation: (a) low ΔK range and (b) intermediate ΔK range.

obtained through low cycle fatigue, and the monotonic value, ε_f, were used in the testing of the growth law. At low ΔK ranges the values of α, in units of length$^{-S/2}$, and S behaved similarly to the values of A and m for Paris law. The values of α and S for the underaged and double aged conditions did not agree as closely as the values of A and m did, but they were still closer to one another than they were to the values for the overaged condition. The same trend was observed whether ε_f or ε_f' was used. α and S for the intermediate ΔK range also acted similarly to the values for A and m for this stress intensity range. The values for S were the same, or very close in two cases, for the equation whether ε_f or ε_f' was employed for the fracture strain. The value of α changed by a factor of $(\varepsilon_f'/\varepsilon_f)$. The use of the low cycle fatigue parameter, ε_f' does not appear to give an improved crack growth prediction, as can be seen in Figures 14 through 16, but just changes the value of α, and in two cases the value of S. Figure 27 shows plots of α vs. S for both ΔK ranges and both ε_f and ε_f'.

The equations with a variable exponent for ΔK, i.e. Paris' and Antolovich's, predict the crack growth rates very accurately for both ΔK ranges investigated. The variable exponent allows for crack growth variations due to differing microstructures rather than being allowed to vary only as other material parameters, e.g. σ_{ys} and ε_f, vary. The two work hardening models fail to predict accurately the observed crack growth rates in age-hardenable aluminum alloys.

The values of A and α, in the low ΔK region, vary inversely with respect to the values of C, n', and ε_f'. The value of S in

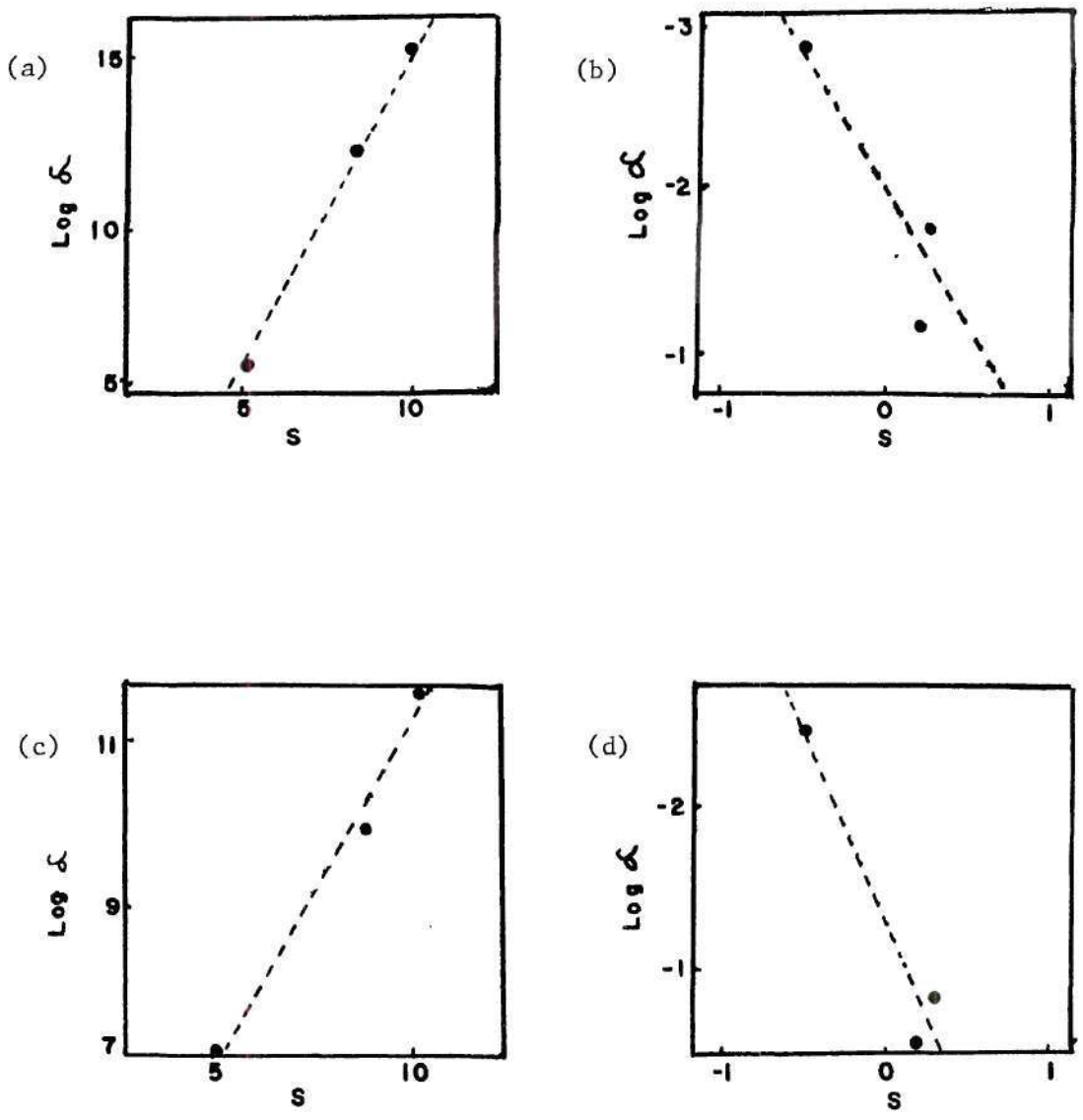

Figure 27. Relationship Between the Parameters α and S of the Antolovich Equation: (a) low ΔK range using ε_f, (b) intermediate ΔK range using ε_f, (c) low ΔK range using ε_f', and (d) intermediate ΔK range using ε_f'.

Antolovich's equation varies inversely with respect to the same variables. The values of ρ and ε_y' predicted by the Head equation, are not accurate enough to precisely predict the crack growth rates observed and are not able to be reliably compared with the low cycle fatigue parameters.

Equations such as Paris' and Antolovich's predict the crack growth rate with a high degree of accuracy assuming that the values of A, α, m and S are known for each alloy and each heat treatment. However, the equations are of no use unless previous crack propagation and low cycle fatigue tests have been conducted on the exact conditions desired. An equation predicting crack rates with the accuracy of these equations, but having a coefficient and exponent which are material constants, and are the same for all aging treatments of the alloy, is desirable.

CHAPTER VI

CONCLUSIONS

1. The effect of microstructure on the fatigue crack growth rates at low ΔK values is not apparent when comparing the underaged and double aged to near maximum strength conditions. The overaged condition exhibits better fatigue resistance in this ΔK range.
2. In the intermediate ΔK test range no obvious crack rate differences are noticeable; thus the microstructure has no rate controlling function at intermediate ΔKs.
3. The better fatigue resistance at low ΔK ranges exhibited by the overaged condition is due to an increased incidence of dislocation looping resulting in more homogeneous deformation.
4. The fatigue crack laws proposed by Paris and Antolovich, which have a variable power for ΔK, predict the crack growth rates with extreme accuracy for both the low and intermediate ΔK ranges for all aging conditions, provided the correct numerical constants are selected. The numerical constants appear to increase as the degree of inhomogeneous deformation increases.
5. Fatigue crack laws based on a strain hardening model, such as the ones proposed by Head and by McClintock, do not predict the crack growth rate accurately.
6. The ranking of the fatigue crack growth parameters A and α is the inverse of the ranking of the low cycle fatigue parameters -C, n' and ε_f' for the low ΔK region.

APPENDIX I

Predicted Crack Growth Rates

Double Aged Condition

ΔK $MNm^{-3/2}$	Observed 10^8 m	Paris 10^8 m	Antolovich 10^8 m	
			Using ε_f	Using ε_f'
6.2	1.4	1.4	1.5	1.5
6.4	2.3	2.3	2.2	2.2
6.5	2.6	2.6	-	2.6
6.6	3.1	3.1	3.1	3.1
6.8	4.3	4.3	4.5	4.5
7.0	6.4	6.4	6.3	6.4
7.2	8.4	8.4	8.9	8.9
7.4	12.5	12.5	12.4	12.4
7.5	15.5	15.5	-	14.6
7.6	17.0	17.0	17.0	17.1
8.0	22.5	22.5	22.7	22.4
9.0	30	30	29.7	29.3
11.0	47	47	46.7	46.4
12.0	57	57	56.8	56.6
13.0	68	68	68.1	68.0
14.0	80	80	80.5	80.6
15.0	94	94	94.1	94.4
16.0	108	108	108.9	109.4
17.0	125	125	124.9	125.7
18.0	145	145	142.1	143.3

Predicted Crack Growth Rates

Double Aged Condition

ΔK $MNm^{-3/2}$	Observed 10^{8} m	Head 10^{8} m	McClintock 10^{8} m	
			$\rho = 10^{-5}$ m	$\varepsilon_y = \varepsilon_{.2\%}$
6.2	1.4	-	-	-
6.4	2.3	-	-	-
6.5	2.6	-	-	-
6.6	3.1	-	-	-
6.8	4.3	-	-	-
7.0	6.4	-	-	-
7.2	8.4	-	-	-
7.4	12.5	-	-	-
7.5	15.5	-	-	-
7.6	17.0	-	-	-
8.0	22.5	.21	23.3	21.9
9.0	30	.26	37.3	35.1
11.0	47	.39	83.1	78.4
12.0	57	.46	117.8	110.0
13.0	68	.54	162.2	152.8
14.0	80	.63	218.1	205.5
15.0	94	.72	287.5	270.9
16.0	108	.82	372.1	350.7
17.0	125	.93	474.3	446.9
18.0	145	1.04	596.1	561.7

Predicted Crack Growth Rates

Underaged Condition

ΔK $MNm^{-3/2}$	Observed 10^{8}m	Paris 10^{8}m	Antolovich 10^{8}m	
			Using ε_f	Using ε_f'
6.6	5.7	5.7	5.5	5.7
6.7	6.8	6.8	6.5	6.7
6.8	8.0	8.0	7.6	7.8
6.9	9.0	9.0	8.8	9.1
7.0	10.0	10.0	10.3	10.6
7.1	11.5	11.5	12.0	12.4
7.2	13.1	13.1	13.9	14.4
7.3	16.0	16.0	16.1	16.6
7.4	19.5	19.5	18.7	19.2
7.5	21.5	21.5	21.6	22.2
8.0	28.5	28.5	28.6	28.6
9.0	34	34	34.1	34.1
10.0	40	40	39.9	39.9
11.0	46	46	46.0	46.0
12.0	52.5	52.5	52.4	52.4
13.0	59	59	59.1	59.1
14.0	66	66	66.0	66.0
15.0	73	73	73.2	73.2
16.0	81	81	83.6	80.6
18.0	96	96	96.2	96.2

Predicted Crack Growth Rates

Underaged Condition

ΔK $MNm^{-3/2}$	Observed 10^{8} m	Head 10^{8} m	McClintock 10^{8} m	
			$\rho = 10^{-5}$ m	$\varepsilon_y = \varepsilon_{.2\%}$
6.6	5.7	-	-	-
6.7	6.8	-	-	-
6.8	8.0	-	-	-
6.9	9.0	-	-	-
7.0	10.0	-	-	-
7.1	11.5	-	-	-
7.2	13.1	-	-	-
7.3	16.0	-	-	-
7.4	19.5	-	-	-
7.5	21.5	-	-	-
8.0	28.5	.08	29.4	21.8
9.0	34	.10	47.1	35.0
10.0	40	.11	71.7	53.3
11.0	46	.14	105.0	78.0
12.0	52.5	.17	148.7	110.5
13.0	59	.20	204.8	152.2
14.0	66	.23	275.5	204.7
15.0	73	.27	363.0	269.8
16.0	81	.31	470.0	349.3
18.0	96	.38	752.8	559.5

Predicted Crack Growth Rates

Overaged Condition

ΔK $MNm^{-3/2}$	Observed 10^8 m	Paris 10^8 m	Antolovich 10^8 m	
			Using ε_f	Using ε_f'
6.6	1.6	1.6	1.6	1.6
6.9	2.2	2.2	2.2	2.1
7.2	2.8	2.8	2.7	2.9
7.5	3.9	3.9	3.8	3.9
7.8	5.0	5.0	5.0	5.1
8.1	6.7	6.7	6.6	6.6
8.4	8.5	8.5	8.5	8.6
8.7	11.0	11.0	10.9	11.0
9.0	14.0	14.0	14.0	14.0
9.3	17.5	17.5	17.5	17.6
10.0	22	22	21.8	21.8
11.0	27	27	26.9	26.9
13.0	39	39	38.9	38.9
14.0	46	46	45.7	45.7
15.0	53	53	53.2	53.2
16.0	61	61	61.4	61.4
17.0	70	70	70.1	70.1
18.0	79	79	79.5	79.5
19.0	90	90	89.6	89.6
19.5	95	95	94.8	94.8

Predicted Crack Growth Rates

Overaged Condition

ΔK $MNm^{-3/2}$	Observed 10^{8} m	Head 10^{8} m	McClintock 10^{8} m	
			$\rho = 10^{-5}$ m	$\varepsilon_y = \varepsilon_{.2\%}$
6.6	1.6	-	-	-
6.9	2.2	-	-	-
7.2	2.8	-	-	-
7.5	3.9	-	-	-
7.8	5.0	-	-	-
8.1	6.7	-	-	-
8.4	8.5	-	-	-
8.7	11.0	-	-	-
9.0	14.0	-	-	-
9.3	17.5	-	-	-
10.0	22	.29	14.2	21.5
11.0	27	.36	20.8	31.4
13.0	39	.50	40.5	61.3
14.0	46	.58	54.5	82.4
15.0	53	.67	71.8	108.6
16.0	61	.76	93.0	140.6
17.0	70	.86	118.5	179.2
18.0	79	.96	148.9	225.2
19.0	90	1.07	184.9	279.6
19.5	95	1.13	205.1	310.2

BIBLIOGRAPHY

1. D. Walton and E.G. Ellison: Int. Met. Reviews, 1972, vol. 17, p. 100.

2. R. J. Selines: Ph. D. Thesis, 1974, Massachusetts Institute of Technology, Cambridge, Mass.

3. W. G. Truckner, J. T. Staley, R. J. Bucci, and A. B. Thakker: "Effects of Microstructure on Fatigue Crack Growth of High-Strength Aluminum Alloys," Alcoa Technical Report, August, 1976.

4. M. Nageswararao, V. Gerold and G. Kralik: "Factors Leading to Grain Boundary Fatigue Crack Propagation in Al-Zn-Mg Alloys," in press.

5. T. H. Sanders: Ph. D. Thesis, 1974, Georgia Institute of Technology, Atlanta, Ga.

6. R. E. Sanders, Jr: M.S. Thesis, 1976, Georgia Institute of Technology, Atlanta, Ga.

7. R. G. Forman, V. E. Kearney, and R. M. Engle: J. Bas. Engr., 1967, p. 459.

8. C. T. Hahn and R. Simon: Engr. Fract. Mech., 1973, vol. 5, p. 523.

9. R. P. Wei: Int. J. of Fract. Mech., 1968, vol. 4, Nr. 2.

10. A. Hartman: Int. J. of Fract. Mech., 1965, vol. 1, p. 167.

11. T. Broom and A. J. Nicholson: J. Inst. Metals, 1960, vol. 9, p. 183.

12. S. M. El-Soudani and R. M. Pelloux: Met. Trans., 1973, vol. 4, p. 519.

13. R. J. Donahue, H. McI. Clark, P. Atanmo, R. Kumble, and A. J. McEvily: Int. J. of Fract. Mech., 1972, vol. 8, p. 209.

14. R. W. Lardner: Phil. Mag., 1968, vol. 17, p. 71.

15. J. Weertman: Proc. 1st Int. Conf. Fract., 1965, Sendai, Japan.

16. R. M. Pelloux: Engr. Fract. Mech., 1970, vol. 1, p. 697.

17. J. P. Hickerson, Jr. and R. W. Hertzberg: Met. Trans., 1972, vol. 3, p. 179.

18. T. Kanazawa, S. Machida, and K. Itoga: Engr. Fract. Mech., 1975, vol. 7, p. 445.

19. C. M. Hudson and J. T. Scardina: Engr. Fract. Mech., 1969, vol. 1, p. 429.

20. N. E. Frost and J. R. Dixon: Int. J. Fract. Mech., 1967, vol. 3, p. 301.

21. W. G. Clark, Jr. and S. J. Hudak, Jr: J. Test. and Eval., 1975, vol. 3, No. 6, p. 454.

22. B. Tomkins: Phil Mag., 1968, vol. 18, p. 1041.

23. P. J. E. Forsyth: The Physical Basis of Metal Fatigue, American Elsevier Publ. Co., New York, 1969, p. 143.

24. A. J. McEvily: "Effect of Constituent Particles on the Notch Sensitivity and Fatigue Crack Propagation Characteristics in Al-Zn-Mg Alloys," Technical Report NASA TD D328, 1962.

25. J. Kershaw: Int. J. Fract. Mech., 1971, vol. 7, p. 269.

26. D. S. Thompson and R. E. Zinkhan: "Research on Synthesis of High-Strength Aluminum Alloys," Technical Report AFML-TR-74-129, Part 1.

27. K. H. Schwalbe: Engr. Fract. Mech., 1974, vol. 6, p. 325.

28. E.T. Wessel: Engr. Fract. Mech., 1968, vol. 1, p. 77.

29. P. C. Paris, M. P. Gomez, and W. E. Anderson: The Trend in Engineering, University of Washington, 1961, vol. 13, p. 9.

30. S. Pearson: Engr. Fract. Mech., 1972, vol. 4, p. 9.

31. A. K. Head: Phil. Mag., 1953, vol. 44, Nr. 354, p. 925.

32. F. A. McClintock: Fracture of Solids, D. C. Drucker and J. J. Gilman, eds., Wiley and Sons, New York, 1963, p. 65.

33. D. S. Dugdale: J. Mech. Phys. Sol., 1960, vol. 8, p. 100.

34. J. R. Rice: ASTM STP 415 (1966).

35. F. Erdogan: Fracture: An Advanced Treatise, vol. 2, Academic Press, New York, 1968, p. 497.

36. S. Ikeda, Y. Izumi, and M. E. Fine: "Plastic Work During Fatigue Crack Propagation in a High Strength Low Alloy Steel and in 7050 Al. Alloy," in press.

37. S. D. Antolovich and A. Saxena: Engr. Fract. Mech., 1975, vol. 1, p. 649.

38. L. P. Pook and N. E. Frost: Metal Fatigue, Clarendon Press, Oxford, England, 1974.

39. P. J. E. Forsyth: Crack Propagation Symposium, Cranfield, England, 1961.

40. V. S. Ivanova: Met. and Fuels, Translation Nr. 3, 1961, vol. 3, p. 77.

41. P. J. E. Forsyth: Acta Met, 1963, vol. 11, p. 703.

42. V. Gerold: X-Ray Small Angle Scattering, ed. H. Brumberger, Gordon and Breuch, New York, 1967, p. 277.

43. T. H. B. Sanders, Jr. and E. A. Starke, Jr.: Met. Trans., 1976, vol. 7, p. 1407.

44. R. E. Sanders, Jr. and E. A. Starke, Jr.: Mat. Sci. and Engr., in press.

45. C. E. Feltner and P. E. Beardmore: ASTM STP 467, 1970.

46. J. C. Grosskreutz and G. G. Shaw: ASTM STP 415, 1967.

47. J. H. Weber and R. W. Hertzberg, Met. Trans., 1971, vol. 2, p. 3498.